Full title: A set of *Arabidopsis* genes involved in the accommodation of the downy mildew pathogen *Hyaloperonospora arabidopsidis*

Short title: A set of *Arabidopsis* genes involved in the interaction with *Hpa*

Martina Katharina Ried[1, #,§], Aline Banhara[1,#], Fang-Yu Hwu[1], Andreas Binder[1], Andrea A. Gust[2], Caroline Höfle[3], Ralph Hückelhoven[3], Thorsten Nürnberger[2], and Martin Parniske[1,*]

[1] University of Munich (LMU), Faculty of Biology, Genetics, Großhaderner Str. 2-4, 82152 Martinsried, Germany

[2] University of Tübingen, Center for Plant Molecular Biology, Plant Biochemistry, Auf der Morgenstelle 32, 72076 Tübingen, Germany

[3] Technical University of Munich, TUM School of Life Sciences Weihenstephan, Phytopathology, Emil-Ramann-Str. 2, 85354 Freising, Germany

[#] Authors contributed equally

[*] Correspondence: Martin Parniske; e-mail: parniske@lmu.de; Phone: +49 (0)89 / 2180-74700

[§] Current address: University of Geneva, Structural Plant Biology Laboratory, Department of Botany and Plant Biology, 30 Quai Ernest Ansermet, 1211 Geneva, Switzerland

Abstract

The intracellular accommodation structures formed by plant cells to host arbuscular mycorrhiza fungi and biotrophic hyphal pathogens are cytologically similar but it remains unclear whether these interactions build on an overlapping genetic framework. In legumes, the malectin-like domain leucine-rich repeat receptor kinase SYMRK, the cation channel POLLUX and members of the nuclear pore NUP107-160 subcomplex are essential for symbiotic signal transduction and arbuscular mycorrhiza development. Here we identified members of these three groups in *Arabidopsis thaliana* and explored their impact on the interaction with the oomycete downy mildew pathogen *Hyaloperonospora arabidopsidis (Hpa).* We report that mutations in the corresponding genes reduced the reproductive success of *Hpa* as determined by sporangiophore and spore counts. We discovered that a developmental transition of haustorial shape occurred significantly earlier and at higher frequency in the mutants. Analysis of the multiplication of extracellular bacterial pathogens, *Hpa*-induced cell death or callose accumulation, as well as *Hpa*- or flg22-induced defence marker gene expression, did not reveal any traces of constitutive or exacerbated defence responses. These findings point towards an overlap between the plant genetic toolboxes involved in the interaction with biotrophic intracellular hyphal symbionts and pathogens in terms of the gene families involved.

Author Summary

Our work reveals genetic commonalities between biotrophic intracellular interactions with symbiotic and pathogenic hyphal microbes. The majority of land plants engages in arbuscular mycorrhiza (AM) symbiosis with phosphate-acquiring arbuscular mycorrhizal fungi to avoid phosphate starvation. Nutrient exchange in this interaction occurs via arbuscules, tree-shaped fungal structures, hosted within plant root cells. A series of plant genes including the Symbiosis Receptor-like kinase (SYMRK), members of the NUP107-160 subcomplex and nuclear envelope localised cation channels are required for a signalling process leading to the development of AM. The model plant *Arabidopsis thaliana* lost the ability to form

AM. Although the ortholog of SYMRK was deleted during evolution, members of the malectin-like domain leucine-rich repeat receptor kinases (MLD-LRR-RKs) gene family, components of the NUP107-160 subcomplex, and an ortholog of the nuclear envelope-localized cation channel POLLUX, are still present in the *Arabidopsis* genome, and *Arabidopsis* leaf cells retained the ability to accommodate haustoria, presumed feeding structures of the obligate biotrophic downy mildew pathogen *Hyaloperonospora arabidopsidis*. We discovered that both of these plant-microbe interactions utilize a corresponding set of genes including the ortholog of POLLUX, members of the NUP107-160 subcomplex and members of the MLD-LRR-RK gene family, thus revealing similarities in the plant program for the intracellular accommodation of biotrophic organisms in symbiosis and disease.

INTRODUCTION

Most land plant species feed carbon sources to arbuscular mycorrhiza (AM) fungi, which in turn deliver phosphate and other nutrients via finely branched intracellular structures called arbuscules [1]. The accommodation of fungal symbionts inside living plant cells involves substantial developmental reprogramming of the host plant cell, initiated by the formation of the pre-penetration apparatus, a transvacuolar cytoplasmic bridge that guides the fungal invasion path [2,3]. The oomycete downy mildew pathogen *Hyaloperonospora arabidopsidis* (*Hpa*) develops intracellular feeding organs, so called haustoria, which exhibit certain structural similarities to the arbuscules of AM fungi [4]. Like arbuscules, haustoria are accommodated inside plant cells and are entirely surrounded by a plant-derived membrane, which keeps the pathogen physically outside the host cytoplasm [5–10]. Structural and functional similarities between accommodation structures for intracellular microbes raised the hypothesis that the corresponding symbiotic and pathogenic associations rely on a similar or even overlapping genetic program [4]. This would imply that filamentous hyphal pathogens exploit an Achilles heel, the presence of the symbiotic program in most land plant species, for their own parasitic lifestyle [11].

In the present study, we tested this hypothesis by focussing on an ancient genetic program comprising the common symbiosis genes (CSGs) [12], which is conserved among angiosperms for the intracellular accommodation of AM fungi [13,14]. In legumes and actinorhizal plants, the CSGs are also required for root nodule symbiosis (RNS) with nitrogen-fixing rhizobia or actinobacteria, respectively [15–17]. In the legume *Lotus japonicus*, the products of some of the CSGs including the MLD-LRR-RK Symbiosis Receptor-like Kinase SYMRK [16,18–20] as well as the nuclear-envelope localised cation channel POLLUX [21,22], are implicated in a signal transduction pathway leading from the perception of microbial signalling molecules at the plasma membrane to the induction of calcium oscillations in and around the nucleus (calcium-spiking), which finally results in the transcriptional activation of symbiosis-related genes and a developmental reprogramming of the respective host cells [1,23]. Furthermore, the nucleoporins NUP85, NUP133 and SEC13 homolog (SEH1) of the NUP107-160 subcomplex are important for the proper establishment of RNS and AM symbiosis [24–27]. The NUP107-160 complex has been implicated in the transport of membrane proteins to the inner membrane of the nuclear envelope [28]. It has been hypothesised that mutations in the NUP107-160 complex may cause a reduced cation channel (e.g. POLLUX) and calcium channel concentration on the inner envelope, which is in accordance with the lack of nuclear calcium spiking in the *NUP107-160* mutants (Jean-Michel Ané, personal communication).

Arabidopsis thaliana belongs to the Brassicaceae, a plant lineage that lost specific CSGs and with this the ability to establish AM symbiosis after the divergence of the Brassicales [29–31]. *A. thaliana* can, however, establish a compatible interaction with the hyphal pathogen *Hpa.* The striking similarities between arbuscules and haustoria led us to investigate whether the interaction of *A. thaliana* with *Hpa*, the fungal powdery mildew pathogen *Erysiphe cruciferarum*, which forms intracellular haustoria in *A. thaliana* epidermal leaf cells, or the extracellular bacterial pathogen *Pseudomonas syringae* rely on a similar gene set as the interaction of plants with beneficial hyphal microbes.

RESULTS

A. thaliana SNUPO mutants reduce the reproductive success of *Hpa*

We inspected the *A. thaliana* genome for the presence of genes related to those required for the interaction with beneficial microbes. Several of the orthologs of key genes required for AM, for example *SYMRK*, *CCaMK* and *CYCLOPS*, are specifically deleted from the *A. thaliana* genome [14,29–32], and thus inaccessible for analysis in the context of the *A. thaliana* interaction with *Hpa*. However, we identified the ortholog of nuclear-localised cation channel *POLLUX* and members of the NUP107-160 subcomplex (S1 + S2 Fig.; Table S1). Furthermore, we identified candidate genes belonging to the MLD-LRR-RK family as close relatives of *LjSYMRK* [16], which we consequently named *SYMRK-homologous Receptor-like Kinase* 1 (*ShRK1*) and *ShRK2* (S1 Fig., S2 Fig., S3 Fig., S4 Fig.; Table S1).

Lines carrying insertional mutant alleles of ***S**hRKs*, selected members of the **NU**P107-160 subcomplex, and the *Arabidopsis* ortholog of ***PO**LLUX* (SNUPO genes) were analysed for their phenotype in the interaction with *Hpa*. In *pollux*, *shrk1*, *shrk2*, the *shrk1* x *shrk2* double mutant, as well as a reference line with a T-DNA insertion in *Phytosulfokine Receptor 1* (*pskr1)* [33,34] or a reference line with an EMS-induced mutation in *Constitutive expression of PR genes 5* (*cpr5*) [35], the reproductive success of *Hpa* isolate NoCo2 - measured as sporangiophore number per cotyledon or spore production - was significantly reduced compared to wild-type plants (Fig. 1 a + c; S5 Fig.).

We analysed a range of NUP107-160 subcomplex members and found that the *sec13* and *nup133* single mutants and the *sec13* x *nup133* double mutant impaired *Hpa* reproductive success (Fig. 1 a + c; S5 Fig.), while lines with T-DNA insertions in *nup43*, *nup85*, *nup160* and *seh1* did not (Fig. 1 b).

All SNUPO genes analysed are constitutively expressed in *Arabidopsis* leaves, in epidermal and mesophyll cells with no consistent clear up- or downregulation in the context of *Hpa* infection [36,37]. The reduced *Hpa* reproductive success could not be explained by a decreased frequency of haustoria

formation measured as percentage of host cells contacted by hyphae that harbour an haustorium. Other than a slight decrease in *pollux*, the frequency in the other mutants was indistinguishable from the wild-type (S6 Fig.).

A. thaliana SNUPO mutants display a significantly higher frequency of multilobed *Hpa* haustoria

However, all *A. thaliana* SNUPO mutants, but not *nup43*, *nup85*, *nup160* and *seh1* mutants, exhibited a significant shift in the ratio of haustoria morphologies (Fig. 2; S7 Fig.). At 5 days post infection (dpi) the majority of haustoria in leaves of the wild-type had a globular, single-lobed appearance. Deviations from such morphology, typically characterised by multiple lobes on a single haustorium ("multilobed"), were observed as well. The amount of multilobed haustoria in the SNUPO mutants was significantly increased, a phenomenon that was alleviated in the tested complementation lines (Fig. 2 a + b). In contrast to the SNUPO mutants, the disease resistant *pskr1* mutant did not show any signs of altered haustoria development (Fig. 2 a). In both, wild-type and *shrk1* x *shrk2*, the percentage of multilobed haustoria increased over time, but was significantly higher in *shrk1* x *shrk2* at each analysed time point (Fig. 2 d). To test whether multilobed haustoria are the result of the harsh chemical clearance of the leaf and trypan blue staining procedure, we visualised the haustoria shape *in vivo*. We made use of a stable transgenic *A. thaliana* line expressing RPW8.2-YFP [38] (Fig. 2) and could confirm that multilobed haustoria appeared already in living plant cells (Fig. 2).

ios1 mutants of ecotypes Ler and Col-0 differ in the frequency of multilobed haustoria

L. japonicus SYMRK belongs to the LRR I-RK family of receptor kinases, which consists of 50 members in *A. thaliana* [39,40]. Of these, *Impaired Oomycete Susceptibility 1* (*IOS1*) has been implicated in defence-related signalling [40,41]. On the one hand, *IOS1* supports the infection of an obligate biotrophic oomycete pathogen, but on the other hand, is important for the resistance against bacteria [40,41]. Interestingly, we could only observe enhanced frequency of multilobed haustoria in an *ios1* mutant of

the *A. thaliana* ecotype Ler but not in an *ios1* mutant of Col-0, which might imply that different paralogs are important for plant-microbe interaction in different ecotypes (S8 Fig.).

The reproductive success of a powdery mildew pathogen appears unaltered on *A. thaliana* SNUPO mutant leaves

To investigate the specificity of the role of SNUPO genes in plant-pathogen interactions, we infected SNUPO mutants with the haustoria-forming powdery mildew fungus *E. cruciferarum*. We did not observe a consistent reduction in the reproductive success of *E. cruciferarum* (Fig. 3; S9 Fig.). A morphological comparison of haustoria shape was not attempted because of the much more complex and highly variable haustoria morphology in this interaction.

***A. thaliana* SNUPO mutants do not exhibit constitutive or exacerbated activation of defence responses**

Plant evolution resulted in several defence strategies against microbial pathogens. For example, PAMP triggered immunity (PTI) is initiated by the perception of pathogen-associated molecular patterns (PAMPs) or plant-derived damage-associated molecular patterns (DAMPs) and results in plant defence responses accompanied by the activation of defence marker genes or callose deposition [42]. To analyse whether the increased *Hpa* resistance of the SNUPO mutants is a result of deregulated defence responses, we investigated the basal transcript levels of the three PAMP-induced marker genes - *Pathogenesis-Related gene 1* (*PR1*), a marker gene for salicylic acid (SA)-mediated resistance [43], *Ethylene Response Factor 1* (*ERF1*), a marker gene for ethylene-mediated resistance [44] and the plant defensin *PDF1.2a*, a marker gene for jasmonic acid (JA)- and ethylene-mediated resistance [45] in the absence of pathogenic attack. Transcript levels in the tested mutants under non-challenged conditions did not differ from transcript levels in the wild-type (Fig. 4 a, black circles). To examine whether SNUPO mutants show enhanced activation of defence marker genes, we analysed the transcript levels of *PR1*, *ERF1* and *PDF1.2a* in plants infected with *Hpa*. All tested genes were upregulated to a similar extent in the SNUPO

mutants and the wild-type (Fig. 4 a, empty circles). Only *PDF1.2a* transcript levels were significantly lower in *Hpa*-infected *shrk1 x shrk2* plants than in infected wild-type plants, however, it is unlikely that this is the reason for the increased pathogen resistance of the double mutant. Moreover, the ability of *Hpa* to suppress callose deposition around the haustorial neck region [46] was not disturbed in the SNUPO mutants compared to the wild-type (Fig. 4 b).

In addition to the expression levels of defence marker genes, we investigated other symptoms typically associated with deregulated immune responses. We could not observe any developmental or growth defects, which are typically a result of the hyper-activation of the SA-dependent defence pathway [35], in SNUPO mutants grown side-by-side with the wild-type and the dwarf mutant *suppressor of npr1-1, constitutive 1* (*snc1* [47]) (S10 Fig.). Furthermore, we analysed constitutive and *Hpa*-induced cell death responses in SNUPO mutants and the wild-type (Fig. 5). Most of the non-infected leaves did not display any sign of cell death (Fig. 5, first column), but dark-blue stained dead cells were sporadically observed with no significant differences between non-infected leaves of both wild-type and SNUPO mutants (Fig. 5, second column and upper graph). In infected leaves of the SNUPO mutants, cell death is detected in, or adjacent to, haustoria-containing cells in a frequency indistinguishable from or even lower than the wild-type (Fig. 5, third column and lower graph). In all genotypes, infected leaves contain hyphal strands growing in the absence of any cell death (Fig. 5 fourth column).

flg22-induced gene expression and resistance to *P. syringae* is unaltered in *A. thaliana* SNUPO mutants

To examine whether mutation of SNUPO genes has an effect on signalling related to PAMP-triggered immunity, we inspected the transcript levels of *Flg22-induced Receptor-like Kinase 1* (*FRK1* [48]) and *ERF1* in the wild-type, the SNUPO mutants and a *fls2* mutant (Fig. 6) in response to the bacterial flagellin-derived peptide flg22 [49]. Transcript levels in mock-treated samples were not different in the wild-type and the analysed mutants, except for the *shrk1* mutant that displayed a slight increase in basal

FRK1 transcript levels, which was not detectable in the *shrk1 x shrk2* double mutant, and the *nup133 x sec13* double mutants that contained slightly decreased basal levels of *ERF1* transcripts. The deviations observed for individual mutants are unlikely responsible for the increased *Hpa* resistance. Six hours after flg22 treatment the tested genes were all upregulated to the same extent in the SNUPO mutants and the wild-type (Fig. 6 a). Furthermore, we investigated the growth behaviour of *P. syringae* on the wild-type and on SNUPO mutants (Fig. 6 b). *P. syringae* pv. *tomato* (*Pto*) DC3000 induces the activation of SA-dependent defence signalling in the host, and deregulation of this pathways impairs *P. syringae* resistance [50]. The growth of *Pto* DC3000 wild-type or the avirulent *ΔAvrPto/PtoB* strain was unaltered on the *A. thaliana* SNUPO mutants, providing further evidence that they do not exhibit constitutive or enhanced activation of SA-dependent defences (Fig. 6 b).

DISCUSSION

Obligate biotrophic hyphal pathogens like *Hpa* that form haustoria inside living plant cells depend on the vitality of their host cell for their own survival and reproduction. The plant genes and developmental programs of the host that are supporting the formation and maintenance of oomycetal haustoria are largely unexplored. Here we tested the hypothesis that the biotrophic pathogen *Hpa* utilises a gene set related to that enabling intracellular accommodation in the context of AM symbiosis.

SNUPO mutants reveal a link between the timing of haustorial shape shifts and reproductive success

We observed - based on sporangiophore and spore counts - that *A. thaliana* SNUPO mutants are impaired in supporting the reproduction of the oomycete pathogen *Hpa*. This was associated with a shift in the haustoria morphology. Intriguingly, we observed congruent phenotypes in mutants of diverse protein classes with the only connector between these protein classes being their reported involvement in root endosymbioses. The frequency of multilobed haustoria increased in the wild-type as well as in the

mutants over time revealing a clear connection between haustoria morphology and the age of the interaction, which is in line with a previously observed continuous growth of *Albugo* and *Hpa* haustoria over time (Eric Kemen and Marco Thines; independent personal communication). As the frequency of multilobed haustoria was significantly higher in the *A. thaliana* SNUPO mutants at all time points analysed, it appears that haustoria growth is accelerated in the SNUPO mutants. It has been postulated that haustoria are the main avenue for nutrient acquisition from the host [51]. Considering the agricultural impact of biotrophic hyphal pathogens, surprisingly little is known about the precise function of haustoria and changes thereof during haustoria development. Senescence of haustoria has been associated with encasement which was discussed to likely reduce their functionality [52]. Therefore, it is possible that the accelerated formation of multilobed haustoria is a sign of senescence and thus directly responsible for the reduction in *Hpa* reproductive success. This scenario would suggest a role of *Arabidopsis* SNUPO genes in maintaining the single lobed, and presumably functional, stage of *Hpa* haustoria. In an opposite scenario, the surface increase from single lobed to multilobed haustoria may benefit the oomycete and the genes under study are involved in delaying the progress of haustoria development into the multilobed stage. However, this scenario is not compatible with the reduced sporangiophore and spore count on the mutants.

SNUPO mutants exhibit no traces of altered plant defence responses or regulation

Based on the analysis of a wide range of defence symptoms in the classical PTI assays and three different pathosystems, we conclude that *A. thaliana* SNUPO mutants display unaltered levels and frequencies of defence responses. Consequentially, the impairment of the *Hpa* interaction is not due to deregulated defence in these mutants.

***Arabidopsis* SNUPO mutants are specifically impaired in the *Hpa* interaction**

We were unable to detect differences in the interaction of *A. thaliana* SNUPO mutants with the haustoria-forming powdery mildew fungus *E. cruciferarum* in comparison to wild-type plants. This may be due to

the different cell types targeted by *Hpa* and *E. cruciferarum* for haustoria formation. *Hpa* initially colonizes epidermal cells and then progresses to the mesophyll [53], in which the vast majority of haustoria are formed, while *E. cruciferarum* forms haustoria solely within epidermal cells [54]. In addition, the genetic requirements for the intracellular accommodation of fungal and oomycete pathogens may differ. The *A. thaliana Mildew resistance Locus O* (*MLO)* gene, for instance, is an epidermal compatibility factor required for powdery mildew fungus penetration [55], with no role in the *Hpa* interaction reported to date. However, it should be noted that the haustoria of *E. cruciferarum* are structurally very complex and irregularly shaped. Because of this inherent polymorphy, it is possible that we missed subtle structural changes caused by the SNUPO mutations.

Genetic overlaps between symbiotic and pathogen biotrophic interactions

In contrast to the vast knowledge on genes contributing to disease resistance, relatively few genes have been identified that facilitate pathogen colonization on *Arabidopsis*, such as *PMR4*, *PMR5*, *PMR6* [56–58], *DMRs* [59,60], *MYB3R4* [36], and *IOS1* [40]. While *dmr3* and *dmr6* mutants also exhibited aberrantly shaped haustoria, these mutants strongly differ from the consistent phenotype of the SNUPO mutants. In *dmr6*, oomycete growth is arrested after the formation of the first haustoria and the expression of several defence-related genes is elevated in unchallenged *dmr6* mutants [59,60]. *Dmr3* mutants are more resistant to the bacterial pathogen *P. syringae* pv. *tomato,* they exhibit elevated *PR1* expression, and *dmr3* and *dmr6* mutants show increased resistance to the powdery mildew pathogen *Golovinomyces orontii* [59]. Taken together, *dmr3* and *dmr6* mutants confer broad-spectrum resistance and display perturbed defence-related gene expression [59,60]; these data suggest that *DMR3* and *DMR6* – in contrast to *Arabidopsis* SNUPO genes - are rather involved in general plant disease resistance than in compatibility with and the accommodation of a hyphal organism.

It is a long-standing hypothesis that plant pathogens exploit an Achilles heel of the plant, genetic pathways for the intracellular accommodation of mutualistic symbionts such as AM fungi or nitrogen-

fixing bacteria [4,11]. Recently the oomycete pathogen *Phytophthora palmivora*, which forms haustoria that only last for a few hours, has emerged as a hemi-biotrophic model system in two independent laboratories to test this hypothesis in legume mutants. This pathogen quickly progresses to a necrotrophic phase and structural alterations in haustoria development are thus less likely to affect pathogen fitness [61–64]. Huisman and colleagues did not detect any alterations in the infection of *Medicago truncatula* mutant roots of the CSGs *DMI1*, *DMI3* and *IPD3* by *P. palmivora* [64]. Considering that the lifetime of infected cells in the *P. palmivora* interaction is reduced, it appears that the transient biotrophic phase of *P. palmivora* is too short and progresses too fast into the necrotrophic phase to allow the haustorial maintenance functions of the CSGs – or a related gene set - to take effect [65,66]. Therefore, the beneficial effect of these genes or their homologs for hyphal pathogens may only be detectable in longer lasting biotrophic relationships. The too short lifetime of the host cell may also explain the absence of a detectable phenotype in *A. thaliana* SNUPO mutants and *L. japonicus* CSG mutants infected with the beneficial fungus *Piriformospora indica* [67]. Colonisation with the endophytic fungus *Colletotrichum tofieldiae*, is controlled by the plant phosphate starvation response system and *C. tofieldiae* only increases plant fertility and promotes plant growth under phosphorus-limiting conditions [68]. It will be an interesting task of future research to investigate whether *Arabidopsis* SNUPO genes are implicated in the interaction with this beneficial microbe. In contrast, for the symbiosis genes for which a mutant phenotype has been described - namely *RAM2* and *RAD1* - the mutation was not affecting haustoria structure [61–63]. Mutants in the glycerol-phosphate acyl-transferase gene *RAM2* of the model legume *M. truncatula*, for example, had a reduced abundance of small cutin monomers and did not elicit the formation of appressoria by *P. palmivora* at the surface of roots and caused an altered infection behaviour of the AM fungus within the root cortex [63]. This observation also implies that a compatibility factor can be exploited by microbial pathogens and, likewise, by beneficial symbionts. Similarly, mutants of the GRAS protein gene *RAD1*, share a role in AM symbiosis and the *P. palmivora* interaction [61].

Our data revealed genetic commonalities of symbiosis and disease in the formation of intracellular accommodation structures at a later developmental stage of the plant-microbe association. A key difference between our study and the previous ones that failed to observe a mutant phenotype in pathogenic interactions is the longer lasting biotrophic phase in the *A. thaliana* - *Hpa* interaction. Although strongly suggested by the function of the CSGs, it remains unclear whether *A. thaliana* SNUPO genes are similarly involved in a signal transduction pathway directly supporting oomycete development. It will be therefore interesting to identify the mechanistic commonalities between symbiotic and pathogenic interactions with hyphal organisms that are controlled by corresponding gene sets.

Retention of SNUPO genes in the *Arabidopsis* genome

The loss of AM symbiosis in *A. thaliana* and in four other independent plant lineages was correlated with the absence of more than 100 genes with potential roles in AM [29–31,69]. While the exploitation of symbiotic programs by pathogens might explain the consistent deletion of CSGs from five independent plant lineages, it raises the question, which evolutionary forces retained SNUPO genes in the *Arabidopsis* genome. A housekeeping function was not revealed since no pleiotropic developmental phenotypes were observed in the mutants. While, it might be possible that these genes limit *Hpa* colonisation, thereby forcing the oomycete to sporulate earlier or more profusely, our results leave us with the unexpected finding that the only detected role for the SNUPO genes in *A. thaliana* is the support of an oomycete. It will be interesting to find out whether ecological conditions exist, under which oomycete colonization might provide a selective advantage to the host plant, or whether SNUPO genes are also involved in the accommodation of beneficial microbes like *C. tofieldiae* justifying their retention in the *Arabidopsis* genome [70].

MATERIALS AND METHODS

Seed sterilization and plant growth

All *A. thaliana* mutants described in the manuscript were of Col-0 ecotype, except for *ios1*, which was either of Col-0 or Ler ecotype. Seeds were obtained from "The Nottingham Arabidopsis Stock Centre" - NASC [71] or the GABI-DUPLO double mutant collection [72]. For *in vitro* experiments, *A. thaliana* seeds were sterilized by incubation in sterilisation solution (70% ethanol, 0.05% Tween20) for 5 min, followed by incubation in 100% ethanol for 2 min. For *Hpa* infection, seeds were directly germinated in soil and grown for two weeks under long day conditions (16 h light, 22°C, 85 µmol m^{-2} s^{-1}). For *E. cruciferarum* inoculation, plants were grown in a 2:1 soil/sand mixture. Seeds were stratified for 48 h at 4°C prior to transfer into a growth chamber (10 h light, 120 µmol m^{-2} s^{-1} light, 22°C day, 20°C night, 65% relative humidity). For elicitor treatment, seeds were placed on half-strength MS plates [73], stratified for 48 h at 4°C in the dark, and grown for 8 days under long day conditions (16 h light, 23°C, 85 µmol m^{-2} s^{-1}).

A. thaliana stable transformation

Floral dipping of *A. thaliana* was performed as described previously [74].

Pathogen assays and phenotypic analyses

To collect spores for inoculation, *A. thaliana* wild-type (Col-0 or Ler) leaves with sporulating *Hpa* isolate NoCo2 or *Hpa* isolate Waco9, respectively, were harvested seven days post inoculation (dpi) and placed into 10 ml deionized H_2O and vortexed for 2 s in 15 ml reaction tubes. The spore suspension was then filtered through a Miracloth filter and sprayed onto 12-days-old plants using a spraying device. Subsequently, plants were placed into trays and covered with wet translucent plastic lids. Trays were sealed to maintain high humidity, and plants were grown under long day conditions (16 h light, 18°C, 85 µmol $m^{-2}s^{-1}$).

For spore counting, *A. thaliana* wild-type (Col-0) and mutant seedlings were harvested 5 dpi. Ten seedlings per background were harvested into reaction tubes containing 1 ml deionized H_2O and vortexed for 3 min. Spores were counted with a Fuchs Rosenthal chamber. For sporangiophore counting and the investigation of haustoria shape and penetration efficiency cotyledons or leaves were harvested and stained in 0.01% trypan-blue-lactophenol for 3 min at 95°C and 5 h at room temperature, followed by overnight clearing in chloral hydrate (2.5 g/ml). Samples were mounted in glycerol for subsequent differential interference contrast microscopy with a Leica DMI6000B. For sporangiophore counting, a minimum of 50 cotyledons per genotype and replicate were analysed and the number of sporangiophores per infected cotyledon was plotted. For investigation of haustoria shape and penetration efficiency, a minimum of five leaves per genotype and replicate were analysed. On each leaf, the percentage of multilobed haustoria per total haustoria or the percentage of haustoria-containing cells per cells contacted by hyphae was calculated for 10 individual strands of hyphae. On average, 1100 haustoria have been analysed per genotype and experiment. The mean for each leaf was calculated and plotted.

E. cruciferarum was grown on *A. thaliana* wild-type (Col-0) to maintain aggressiveness and on susceptible *phytoalexin deficient 4* (*pad4*) mutants [50] for elevated conidia production. Plants were placed under a polyamide net (0.2 mm^2) and inoculated at a density of 3 - 4 conidia mm^{-2}, by brushing conidia off of *pad4* mutant leaves through the net. Two leaves per plant were harvested, cleared and kept in acetic acid (25%) until microscopic analysis. Leaves were stained in acetic acid (25%) ink (1:9) (Königsblau, Pelikan, 4001), washed in water, placed in water containing a few drops of Tween20, washed in water again, and analysed under a bright-field microscope. For each replicate, conidiophores per colony were counted on 10 colonies per leaf, on 5 - 10 leaves per genotype.

Bacterial strains *Pto* DC3000 or *Pto* DC3000 *ΔAvrPto/AvrPto* were grown and used for infection assays on leaves of 4 - 5 weeks old *A. thaliana* plants as described previously [75,76].

Each experiment was performed at least three times independently.

Observation of haustoria

Leaves of *A. thaliana* wild-type (Col-0) or the *shrk1* x *shrk2* double mutant were harvested at 5 dpi, cleared in 10% KOH for 5 min, stained with 0.05% aniline blue in 67 mM K_2HPO_4 for 20 min and observed with a Leica SP5 confocal light scanning microscope. Images were edited using ImageJ with the "volume viewer" plugin [77].

For Technovit sections, *A. thaliana* wild-type (Col-0) or mutant leaves were infected with *Hpa* as described above and harvested at 7 dpi. Leaves were fixed with 3.7% formaldehyde and dehydrated by incubating samples in 30%, 50%, 70% and 100% ethanol. Samples were embedded in Technovit 7100 according to the manufacturer's instruction. A Leica RM2125 rotary microtome was used to cut 7 µm sections. Sections were stained in 0.01% trypan-blue-lactophenol for 3 h at 37°C, followed by clearing in chloral hydrate (2.5g/ml) and subsequent differential interference contrast microscopy with a Leica DMI6000B.

A. thaliana wild-type (Col-0) plants expressing *RPW8.2-YFP* [38] were infected with *Hpa* as described above, harvested at 10 dpi and observed with a Leica TCS SP 5 confocal laser scanning microscope equipped with a 63x NA 1.2 water-immersion objective.

Analysis of oomycete-associated callose deposition

Oomycete-associated callose deposition was analysed on cotyledons of *A. thaliana* wild-type (Col-0) or SNUPO mutants. Leaves were harvested at 4 dpi, cleared in 10% KOH for 5 min, stained with 0.05% aniline blue in 67 mM K_2HPO_4 for 20 min and mounted in glycerol for observation with a Leica DMI6000B with CFP filter settings. Regions of interest (ROIs) covering the neck bands were selected in ImageJ [77] and the signal intensity of each neck band was calculated from single ROIs and mean intensities were plotted. n = 27 - 72.

Elicitor treatment

For pre-incubation, 8 days old seedlings were transferred to a 12-well plate (3 seedlings/well represent one biological replicate) with half-strength liquid MS medium [73] supplemented with 1% sucrose and incubated overnight under long-day conditions (16 h light, 22°C, 100 µmol m^{-2} s^{-1}; 8 h dark, 18°C) and 100 rpm shaking. On the following day the medium was exchanged, half of the samples were supplemented with 1 µM flg22, and the other half was kept in half-strength MS to serve as mock controls. Plants were then incubated for 6 h at 22°C and 100 rpm shaking. For every genotype, three biological replicates of treated and non-treated samples were harvested and immediately frozen in liquid N_2 for subsequent RNA extraction.

RNA Extraction and qRT-PCR analysis

RNA extraction was performed using the Spectrum™ Plant Total RNA kit (Sigma-Aldrich), followed by DNase I treatment (amplification grade DNase I, Invitrogen™) to remove genomic DNA. First strand cDNA synthesis was performed from 250 ng total RNA using the SuperScript® III First-Strand Synthesis SuperMix (Invitrogen™) with oligo(dT) primers. qRT-PCR was performed in 20 µL reactions containing 1x SYBR Green I (Invitrogen™) in a CFX96 Real-time PCR detection system (Bio-Rad). PCR program: 2'-95°C; 40 x (30''-95°C; 30''-60°C; 20''-72°C); melting curve 95°C – 60°C – 95°C. A primer list can be found in S3 Table. Expression levels of target genes were normalized against the housekeeping genes *TIP41-like* and *PP2A* [78]. For every genotype, three biological replicates represented by two technical duplicates each were analysed.

Gene structure and phylogenetic analyses

Complete annotated genomic sequences were obtained from The *Arabidopsis* Information Resource (TAIR - www.arabidopsis.org) for *A. thaliana*, and from the KDRI website (Kazusa DNA Research Institute, Japan; http://www.kazusa.or.jp/lotus/) and the GenBank for *L. japonicus*. BLAST searches

were performed on TAIR (http://arabidopsis.org/Blast/index.jsp) with the *L. japonicus* genomic CSG sequences as query. The protein domain organization and the exon-intron structure of the *A. thaliana* homologs of *POLLUX*, *SEC13*, *NUP133* (GenBank accession number: KM269292), *ShRK1* and *ShRK2* are identical to that of their *L. japonicus* counterparts. By sequencing a PCR product amplified from *A. thaliana* wild-type (Col-0) cDNA, we demonstrated that, contrary to the TAIR prediction, this was also the case for *NUP133*. The curated sequence has been submitted to TAIR. For phylogenetic studies, protein sequences of *A. thaliana* and *L. japonicus* MLD-LRR-RKs were aligned using MAFFT 7 [79] with default settings. Alignments were used to create phylogenetic trees at the CIPRES web-portal with RAxML 8.2.10 [80] for maximum likelihood analyses. For RAxML, the JTT PAM matrix for amino acid substitutions was chosen.

Statistics and data visualisation

All statistical analyses and data plots have been performed and generated with R version 3.0.2 (2013-09-25) "Frisbee Sailing" [81], using the packages “Hmisc” [82], “car” [83], “multcompView” [84] and “multcomp” [85] or Excel. For statistical analysis, data was either subjected to the nonparametric Wilcoxon-Mann-Whitney test with Bonferroni-Holm correction using Col-0 samples as control group, or was power transformed to improve normality and a one-way ANOVA followed by a Dunnett’s Test with Bonferroni correction was performed using Col-0 samples as control group.

ACKNOWLEDGEMENTS

We thank Ruth Eichmann for performing pilot experiments with *Erysiphe cruciferarum*, Birgit Kemmerling for kindly sending us *pskr-1* seeds, Dirk Metzler for help with statistical analyses and Rosa Elena Andrade Aguirre for help with the phylogenetic analyses.

REFERENCES

1. Gutjahr C, Parniske M. Cell and developmental biology of arbuscular mycorrhiza symbiosis. Annu Rev Cell Dev Biol. 2013;29: 593–617. doi:10.1146/annurev-cellbio-101512-122413

2. Genre A, Chabaud M, Faccio A, Barker DG, Bonfante P. Prepenetration apparatus assembly precedes and predicts the colonization patterns of arbuscular mycorrhizal fungi within the root cortex of both *Medicago truncatula* and *Daucus carota*. Plant Cell. 2008;20: 1407–1420. doi:10.1105/tpc.108.059014

3. Genre A, Chabaud M, Timmers T, Bonfante P, Barker DG. Arbuscular mycorrhizal fungi elicit a novel intracellular apparatus in *Medicago truncatula* root epidermal cells before infection. Plant Cell. 2005;17: 3489–3499. doi:10.1105/tpc.105.035410

4. Parniske M. Intracellular accommodation of microbes by plants: A common developmental program for symbiosis and disease? Current Opinion in Plant Biology. 2000. pp. 320–328. doi:10.1016/S1369-5266(00)00088-1

5. Hückelhoven R, Panstruga R. Cell biology of the plant-powdery mildew interaction. Current Opinion in Plant Biology. 2011. pp. 738–746. doi:10.1016/j.pbi.2011.08.002

6. Mims CW, Richardson EA, Holt III BF, Dangl JL. Ultrastructure of the host-pathogen interface in *Arabidopsis thaliana* leaves infected by the downy mildew *Hyaloperonospora parasitica*. Can J Bot. 2004; doi:10.1139/b04-073

7. Lu YJ, Schornack S, Spallek T, Geldner N, Chory J, Schellmann S, et al. Patterns of plant subcellular responses to successful oomycete infections reveal differences in host cell reprogramming and endocytic trafficking. Cell Microbiol. 2012; doi:10.1111/j.1462-5822.2012.01751.x

8. Holub EB. Natural history of *Arabidopsis thaliana* and oomycete symbioses. The Downy Mildews - Genetics, Molecular Biology and Control. 2008. doi:10.1007/978-1-4020-8973-2_8

9. Coates ME, Beynon JL. *Hyaloperonospora arabidopsidis* as a pathogen model. Annu Rev Phytopathol. 2010; doi:10.1146/annurev-phyto-080508-094422

10. McDowell JM. *Hyaloperonospora arabidopsidis*: A model pathogen of *Arabidopsis*. Genomics of plant-associated fungi and oomycetes: Dicot Pathogens. 2014. doi:10.1007/978-3-662-44056-8_10

11. Evangelisti E, Rey T, Schornack S. Cross-interference of plant development and plant-microbe interactions. Current Opinion in Plant Biology. 2014. pp. 118–126. doi:10.1016/j.pbi.2014.05.014

12. Kistner C, Parniske M. Evolution of signal transduction in intracellular symbiosis. Trends in Plant Science. 2002. pp. 511–518. doi:10.1016/S1360-1385(02)02356-7

13. Gutjahr C, Banba M, Croset V, An K, Miyao A, An G, et al. Arbuscular mycorrhiza-specific signaling in rice transcends the common symbiosis signaling pathway. Plant Cell. 2008;20: 2989–3005. doi:10.1105/tpc.108.062414

14. Yano K, Yoshida S, Muller J, Singh S, Banba M, Vickers K, et al. CYCLOPS, a mediator of symbiotic intracellular accommodation. Proc Natl Acad Sci. 2008;105: 20540–20545. doi:10.1073/pnas.0806858105

15. Gherbi H, Markmann K, Svistoonoff S, Estevan J, Autran D, Giczey G, et al. SymRK defines a common genetic basis for plant root endosymbioses with arbuscular mycorrhiza fungi, rhizobia, and Frankia bacteria. Proc Natl Acad Sci. 2008;105: 4928–4932. doi:10.1073/pnas.0710618105

16. Markmann K, Giczey G, Parniske M. Functional adaptation of a plant receptor-kinase paved the way for the evolution of intracellular root symbioses with bacteria. PLoS Biol. 2008;6: 0497–0506. doi:10.1371/journal.pbio.0060068

17. Svistoonoff S, Benabdoun FM, Nambiar-Veetil M, Imanishi L, Vaissayre V, Cesari S, et al. The Independent acquisition of plant root nitrogen-fixing symbiosis in Fabids recruited the same genetic pathway for nodule organogenesis. PLoS One. 2013;8. doi:10.1371/journal.pone.0064515

18. Stracke S, Kistner C, Yoshida S, Mulder L, Sato S, Kaneko T, et al. A plant receptor-like kinase required for both bacterial and fungal symbiosis. Nature. 2002;417: 959–962. doi:10.1038/nature00841

19. Antolín-Llovera M, Ried MK, Parniske M. Cleavage of the symbiosis receptor-like kinase ectodomain promotes complex formation with Nod Factor Receptor 5. Curr Biol. 2014;24: 422–427. doi:10.1016/j.cub.2013.12.053

20. Ried MK, Antolín-Llovera M, Parniske M. Spontaneous symbiotic reprogramming of plant roots triggered by receptor-like kinases. Elife. 2014;3: 1–17. doi:10.7554/eLife.03891

21. Kanamori N, Madsen LH, Radutoiu S, Frantescu M, Quistgaard EMH, Miwa H, et al. A nucleoporin is required for induction of Ca^{2+} spiking in legume nodule development and essential

for rhizobial and fungal symbiosis. Proc Natl Acad Sci. 2006;103: 359–364. doi:10.1073/pnas.0508883103

22. Alber F, Dokudovskaya S, Veenhoff LM, Zhang W, Kipper J, Devos D, et al. The molecular architecture of the nuclear pore complex. Nature. 2007;450: 695–701. https://doi.org/10.1038/nature06405

23. Saito K, Yoshikawa M, Yano K, Miwa H, Uchida H, Asamizu E, et al. *NUCLEOPORIN85* is required for calcium spiking, fungal and bacterial symbioses, and seed production *in Lotus japonicus*. Plant Cell. 2007;19: 610–624. doi:10.1105/tpc.106.046938

24. Groth M, Takeda N, Perry J, Uchida H, Draxl S, Brachmann A, et al. *NENA*, a *Lotus japonicus* homolog of *Sec13*, is required for rhizodermal infection by arbuscular mycorrhiza fungi and rhizobia but dispensable for cortical endosymbiotic development. Plant Cell. 2010;22: 2509–2526. doi:10.1105/tpc.109.069807

25. Charpentier M, Bredemeier R, Wanner G, Takeda N, Schleiff E, Parniske M. *Lotus japonicus* CASTOR and POLLUX are ion channels essential for perinuclear calcium spiking in legume Root endosymbiosis. Plant Cell. 2008;20: 3467–3479. doi:10.1105/tpc.108.063255

26. Venkateshwaran M, Cosme A, Han L, Banba M, Satyshur KA, Schleiff E, et al. The recent evolution of a symbiotic ion channel in the legume family altered ion conductance and improved functionality in calcium signaling. Plant Cell. 2012;24: 2528–2545. doi:10.1105/tpc.112.098475

27. Oldroyd GED. Speak, friend, and enter: Signalling systems that promote beneficial symbiotic associations in plants. Nature Reviews Microbiology. 2013. pp. 252–263. doi:10.1038/nrmicro2990

28. Meinema AC, Laba JK, Hapsari RA, Otten R, Mulder FAA, Kralt A, et al. Long unfolded linkers facilitate membrane protein import through the nuclear pore complex. Science (80-). 2011; doi:10.1126/science.1205741

29. Favre P, Bapaume L, Bossolini E, Delorenzi M, Falquet L, Reinhardt D. A novel bioinformatics pipeline to discover genes related to arbuscular mycorrhizal symbiosis based on their evolutionary conservation pattern among higher plants. BMC Plant Biol. 2014;14. doi:10.1186/s12870-014-0333-0

30. Delaux PM, Varala K, Edger PP, Coruzzi GM, Pires JC, Ané JM. Comparative phylogenomics

uncovers the impact of symbiotic associations on host genome evolution. PLoS Genet. 2014;10. doi:10.1371/journal.pgen.1004487

31. Bravo A, York T, Pumplin N, Mueller LA, Harrison MJ. Genes conserved for arbuscular mycorrhizal symbiosis identified through phylogenomics. Nat Plants. 2016;2. doi:10.1038/NPLANTS.2015.208

32. Endre G, Kereszt A, Kevei Z, Mihacea S, Kaló P, Kiss GB. A receptor kinase gene regulating symbiotic nodule development. Nature. 2002;417: 962–966. doi:10.1038/nature00842

33. Mosher S, Seybold H, Rodriguez P, Stahl M, Davies KA, Dayaratne S, et al. The tyrosine-sulfated peptide receptors PSKR1 and PSY1R modify the immunity of *Arabidopsis* to biotrophic and necrotrophic pathogens in an antagonistic manner. Plant J. 2013;73: 469–482. doi:10.1111/tpj.12050

34. Matsubayashi Y. Disruption and overexpression of *Arabidopsis Phytosulfokine Receptor* gene affects cellular longevity and potential for growth. Plant Physiol. 2006;142: 45–53. doi:10.1104/pp.106.081109

35. Bowling SA. The *cpr5* Mutant of *Arabidopsis* expresses both *NPR1*-dependent and *NPR1*-independent resistance. Plant Cell. 1997;9: 1573–1584. doi:10.1105/tpc.9.9.1573

36. Chandran D, Inada N, Hather G, Kleindt CK, Wildermuth MC. Laser microdissection of *Arabidopsis* cells at the powdery mildew infection site reveals site-specific processes and regulators. Proc Natl Acad Sci. 2010;107: 460–465. doi:10.1073/pnas.0912492107

37. Wang W, Barnaby JY, Tada Y, Li H, Tör M, Caldelari D, et al. Timing of plant immune responses by a central circadian regulator. Nature. 2011; doi:10.1038/nature09766

38. Wang W, Wen Y, Berkey R, Xiao S. Specific Targeting of the *Arabidopsis* resistance protein RPW8.2 to the interfacial membrane encasing the fungal haustorium renders broad-spectrum resistance to powdery mildew. Plant Cell. 2009;21: 2898–2913. doi:10.1105/tpc.109.067587

39. Shiu S-H, Bleecker AB. Expansion of the receptor-like kinase/Pelle gene family and receptor-like proteins in *Arabidopsis*. Plant Physiol. 2003;132: 530 LP-543. http://www.plantphysiol.org/content/132/2/530.abstract

40. Hok S, Danchin EGJ, Allasia V, Panabières F, Attard A, Keller H. An *Arabidopsis* malectin-like leucine-rich repeat receptor-like kinase contributes to downy mildew disease. Plant, Cell Environ.

2011;34: 1944–1957. doi:10.1111/j.1365-3040.2011.02390.x

41. Yeh Y-H, Panzeri D, Kadota Y, Huang Y-C, Huang P-Y, Tao C-N, et al. The *Arabidopsis* Malectin-Like/LRR-RLK IOS1 is Critical for BAK1-dependent and BAK1-independent pattern-triggered immunity. Plant Cell. 2016;28: 1701–1721. doi:10.1105/tpc.16.00313

42. Jones JDG, Dangl JL. The plant immune system. Nature. 2006;444: 323–329. doi:10.1038/nature05286

43. Ryals J, Neuenschwander U, Willits M, Molina A, Steiner H-Y, Hunt M. Systemic acquired resistance. Plant Cell. 1996;8: 1809–1819. doi:10.4161/psb.1.4.3221

44. Solano R, Stepanova A, Chao Q, Ecker JR. Nuclear events in ethylene signaling: A transcriptional cascade mediated by *ETHYLENE-INSENSITIVE3* and *ETHYLENE-RESPONSE-FACTOR1*. Genes Dev. 1998;12: 3703–3714. doi:10.1101/gad.12.23.3703

45. Penninckx I, Eggermont K, Terras FR, Thomma BP, DeSamblanx GW, Buchala A, et al. Pathogen-induced systemic activation of a plant defensin gene in *Arabidopsis* follows a salicylic acid-independent pathway. Plant Cell. 1996;8: 2309–2323. doi:10.1105/tpc.8.12.2309

46. Sohn KH, Lei R, Nemri A, Jones JDG. The downy mildew effector proteins ATR1 and ATR13 promote disease susceptibility in *Arabidopsis thaliana*. Plant Cell. 2007;19: 4077–4090. doi:10.1105/tpc.107.054262

47. Li X, Clarke JD, Zhang Y, Dong X. Activation of an *EDS1*-Mediated *R*-gene pathway in the *snc1* mutant leads to constitutive, *NPR1*-independent pathogen resistance. Mol Plant-Microbe Interact. 2001;14: 1131–1139. doi:10.1094/MPMI.2001.14.10.1131

48. Asai T, Tena G, Plotnikova J, Willmann MR, Chiu WL, Gomez-Gomez L, et al. Map kinase signalling cascade in *Arabidopsis* innate immunity. Nature. 2002;415: 977–983. doi:10.1038/415977a

49. Chinchilla D, Bauer Z, Regenass M, Boller T, Felix G. The *Arabidopsis* receptor kinase FLS2 binds flg22 and determines the specificity of flagellin perception. Plant Cell. 2006;18: 465–476. doi:10.1105/tpc.105.036574

50. Glazebrook J, Ausubel FM. Isolation of phytoalexin-deficient mutants of *Arabidopsis thaliana* and characterization of their interactions with bacterial pathogens. Proc Natl Acad Sci. 1994;91: 8955–8959. doi:10.1073/pnas.91.19.8955

51. Voegele RT, Struck C, Hahn M, Mendgen K. The role of haustoria in sugar supply during infection of broad bean by the rust fungus *Uromyces fabae*. Proc Natl Acad Sci. 2001;98: 8133–8138. doi:10.1073/pnas.131186798

52. Caillaud MC, Wirthmueller L, Sklenar J, Findlay K, Piquerez SJM, Jones AME, et al. The plasmodesmal protein PDLP1 localises to haustoria-associated membranes during downy mildew infection and regulates callose deposition. PLoS Pathog. 2014;10. doi:10.1371/journal.ppat.1004496

53. Slusarenko AJ, Schlaich NL. Downy mildew of *Arabidopsis thaliana* caused by *Hyaloperonospora parasitica* (formerly *Peronospora parasitica*). Mol Plant Pathol. 2003;4: 159–170. doi:10.1046/j.1364-3703.2003.00166.x

54. Micali C, Göllner K, Humphry M, Consonni C, Panstruga R. The powdery mildew disease of *Arabidopsis*: A paradigm for the interaction between plants and biotrophic fungi. Arab B. 2008;6: e0115. doi:10.1199/tab.0115

55. Consonni C, Humphry ME, Hartmann HA, Livaja M, Durner J, Westphal L, et al. Conserved requirement for a plant host cell protein in powdery mildew pathogenesis. Nat Genet. 2006;38: 716–720. doi:10.1038/ng1806

56. Vogel J, Somerville S. Isolation and characterization of powdery mildew-resistant *Arabidopsis* mutants. Proc Natl Acad Sci. 2000;97: 1897–1902. doi:10.1073/pnas.030531997

57. Vogel JP, Raab TK, Somerville CR, Somerville SC. Mutations in *PMR5* result in powdery mildew resistance and altered cell wall composition. Plant J. 2004;40: 968–978. doi:10.1111/j.1365-313X.2004.02264.x

58. Vogel JP. *PMR6*, a pectate lyase-like gene required for powdery mildew susceptibility in *Arabidopsis*. Plant Cell. 2002;14: 2095–2106. doi:10.1105/tpc.003509

59. Van Damme M, Andel A, Huibers RPRP, Panstruga R, Weisbeek PJPJ, Van den Ackerveken G, et al. Identification of *Arabidopsis* loci required for susceptibility to the downy mildew pathogen *Hyaloperonospora parasitica*. Mol plant-microbe Interact. 2005;18: 583–592. doi:10.1094/MPMI-18-0583.

60. Van Damme M, Huibers RP, Elberse J, Van Den Ackerveken G. *Arabidopsis DMR6* encodes a putative 2OG-Fe(II) oxygenase that is defense-associated but required for susceptibility to downy

mildew. Plant J. 2008;54: 785–793. doi:10.1111/j.1365-313X.2008.03427.x

61. Rey T, Bonhomme M, Chatterjee A, Gavrin A, Toulotte J, Yang W, et al. The *Medicago truncatula* GRAS protein RAD1 supports arbuscular mycorrhiza symbiosis and *Phytophthora palmivora* susceptibility. J Exp Bot. 2017;68: 5871–5881. doi:10.1093/jxb/erx398

62. Rey T, Chatterjee A, Buttay M, Toulotte J, Schornack S. *Medicago truncatula* symbiosis mutants affected in the interaction with a biotrophic root pathogen. New Phytol. 2015;206: 497–500. doi:10.1111/nph.13233

63. Wang E, Schornack S, Marsh JF, Gobbato E, Schwessinger B, Eastmond P, et al. A common signaling process that promotes mycorrhizal and oomycete colonization of plants. Curr Biol. 2012;22: 2242–2246. doi:10.1016/j.cub.2012.09.043

64. Huisman R, Bouwmeester K, Brattinga M, Govers F, Bisseling T, Limpens E. Haustorium formation in *Medicago truncatula* roots infected by *Phytophthora palmivora* does not involve the common endosymbiotic program shared by arbuscular mycorrhizal fungi and rhizobia. Mol Plant-Microbe Interact. 2015;28: 1271–1280. doi:10.1094/MPMI-06-15-0130-R

65. Schoina C, Bouwmeester K, Govers F. Infection of a tomato cell culture by *Phytophthora infestans*; a versatile tool to study *Phytophthora*-host interactions. Plant Methods. 2017;13. doi:10.1186/s13007-017-0240-0

66. Fuechtbauer W, Yunusov T, Bozsóki Z, Gavrin A, James EK, Stougaard J, et al. LYS12 LysM receptor decelerates *Phytophthora palmivora* disease progression in *Lotus japonicus*. Plant J. 2018;93: 297–310. doi:10.1111/tpj.13785

67. Banhara A, Ding Y, Kühner R, Zuccaro A, Parniske M. Colonization of root cells and plant growth promotion by *Piriformospora indica* occurs independently of plant common symbiosis genes. Front Plant Sci. 2015;6: 667. doi:10.3389/fpls.2015.00667

68. Hiruma K, Gerlach N, Sacristán S, Nakano RT, Hacquard S, Kracher B, et al. Root endophyte *Colletotrichum tofieldiae* confers plant fitness benefits that are phosphate status dependent. Cell. 2016; doi:10.1016/j.cell.2016.02.028

69. Delaux PM, Séjalon-Delmas N, Bécard G, Ané JM. Evolution of the plant-microbe symbiotic "toolkit." Trends in Plant Science. 2013. pp. 298–304. doi:10.1016/j.tplants.2013.01.008

70. Salvaudon L, Héraudet V, Shykoff JA. *Arabidopsis thaliana* and the Robin Hood parasite: A

chivalrous oomycete that steals fitness from fecund hosts and benefits the poorest one? Biol Lett. 2008;4: 526–529. doi:10.1098/rsbl.2008.0332

71. Scholl RL, May ST, Ware DH. Seed and molecular resources for *Arabidopsis*. Plant Physiol. 2000;124: 1477–80. doi:10.1104/PP.124.4.1477

72. Bolle C, Huep G, Kleinbölting N, Haberer G, Mayer K, Leister D, et al. GABI-DUPLO: A collection of double mutants to overcome genetic redundancy in *Arabidopsis thaliana*. Plant J. 2013;75: 157–171. doi:10.1111/tpj.12197

73. Murashige T, Skoog F. A revised medium for rapid growth and bio assays with tobacco tissue cultures. Physiol Plant. 1962;15: 473–497. doi:10.1111/j.1399-3054.1962.tb08052.x

74. Clough SJ, Bent AF. Floral dip: A simplified method for *Agrobacterium*-mediated transformation of *Arabidopsis thaliana*. Plant J. 1998;16: 735–743. doi:10.1046/j.1365-313X.1998.00343.x

75. Lin NC, Martin GB. An avrPto/avrPtoB mutant of *Pseudomonas syringae pv. tomato* DC3000 does not elicit Pto-mediated resistance and is less virulent on tomato. Mol Plant-Microbe Interact. 2005;18: 43–51. doi:10.1094/MPMI-18-0043

76. Kemmerling B, Schwedt A, Rodriguez P, Mazzotta S, Frank M, Qamar SA, et al. The BRI1-Associated Kinase 1, BAK1, has a brassinolide-independent role in plant cell-death control. Curr Biol. 2007;17: 1116–1122. doi:10.1016/j.cub.2007.05.046

77. Schneider CA, Rasband WS, Eliceiri KW. NIH Image to ImageJ: 25 years of image analysis. Nature Methods. 2012. pp. 671–675. doi:10.1038/nmeth.2089

78. Czechowski T. Genome-wide identification and testing of superior reference genes for transcript normalization in *Arabidopsis*. Plant Physiol. 2005;139: 5–17. doi:10.1104/pp.105.063743

79. Katoh K. MAFFT: a novel method for rapid multiple sequence alignment based on fast Fourier transform. Nucleic Acids Res. 2002;30: 3059–3066. doi:10.1093/nar/gkf436

80. Stamatakis A, Hoover P, Rougemont J. A rapid bootstrap algorithm for the RAxML web servers. Syst Biol. 2008;57: 758–771. doi:10.1080/10635150802429642

81. R Development Core Team. R: A Language and Environment for Statistical Computing. R Found Stat Comput. 2016; doi:10.1007/978-3-540-74686-7

82. Harrell FEJ. Hmisc: Harrell Miscellaneous. R package version 3.0-12. 2018.

doi:10.1002/14651858.CD001116.pub3.Copyright

83. Fox J, Weisberg S. An R companion to applied regression. SAGE. 2011. doi:10.1177/0049124105277200

84. Graves S, Piepho H-P, Selzer L, with help from Dorai-Raj S. multcompView: Visualizations of paired comparisons. R Packag version 01-5. 2012;46. doi:https://CRAN.R-project.org/package=multcompView

85. Hothorn T, Bretz F, Westfall P. Simultaneous inference in general parametric models. Biometrical Journal. 2008. pp. 346–363. doi:10.1002/bimj.200810425

FIGURES

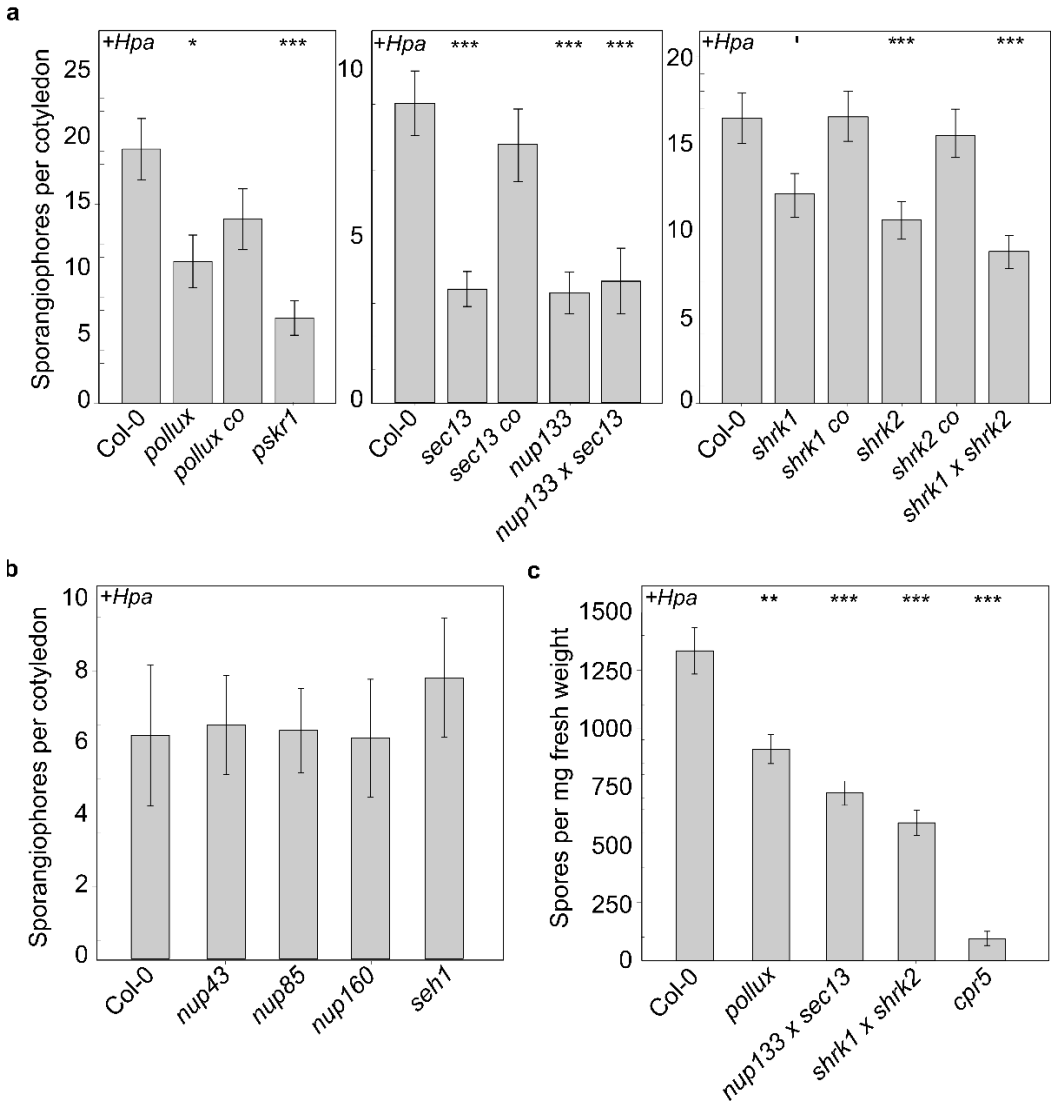

Fig. 1: Mutations in *A. thaliana* SNUPO genes reduce the reproductive success of the oomycete downy mildew pathogen *Hpa*.

(a + b) Bar charts represent the mean number of sporangiophores ± s.e.m on infected cotyledons of *A. thaliana* wild-type (Col-0) or the indicated mutants 4 dpi with *Hpa* isolate NoCo2. n = 14 - 63 **(c)** Bar charts represent the mean number of spores ± s.e.m per mg fresh weight isolated from *A. thaliana* wild-type (Col-0) or the indicated mutants 4 dpi with *Hpa* isolate NoCo2. n = 9. Stars indicate significant differences to Col-0 (Wilcoxon-Mann-Whitney test with Bonferroni-Holm correction; ‘, $p = 0.066$ *, $p < 0.05$; **, $p < 0.01$; ***, $p < 0.001$). Each experiment was performed at least three times independently.

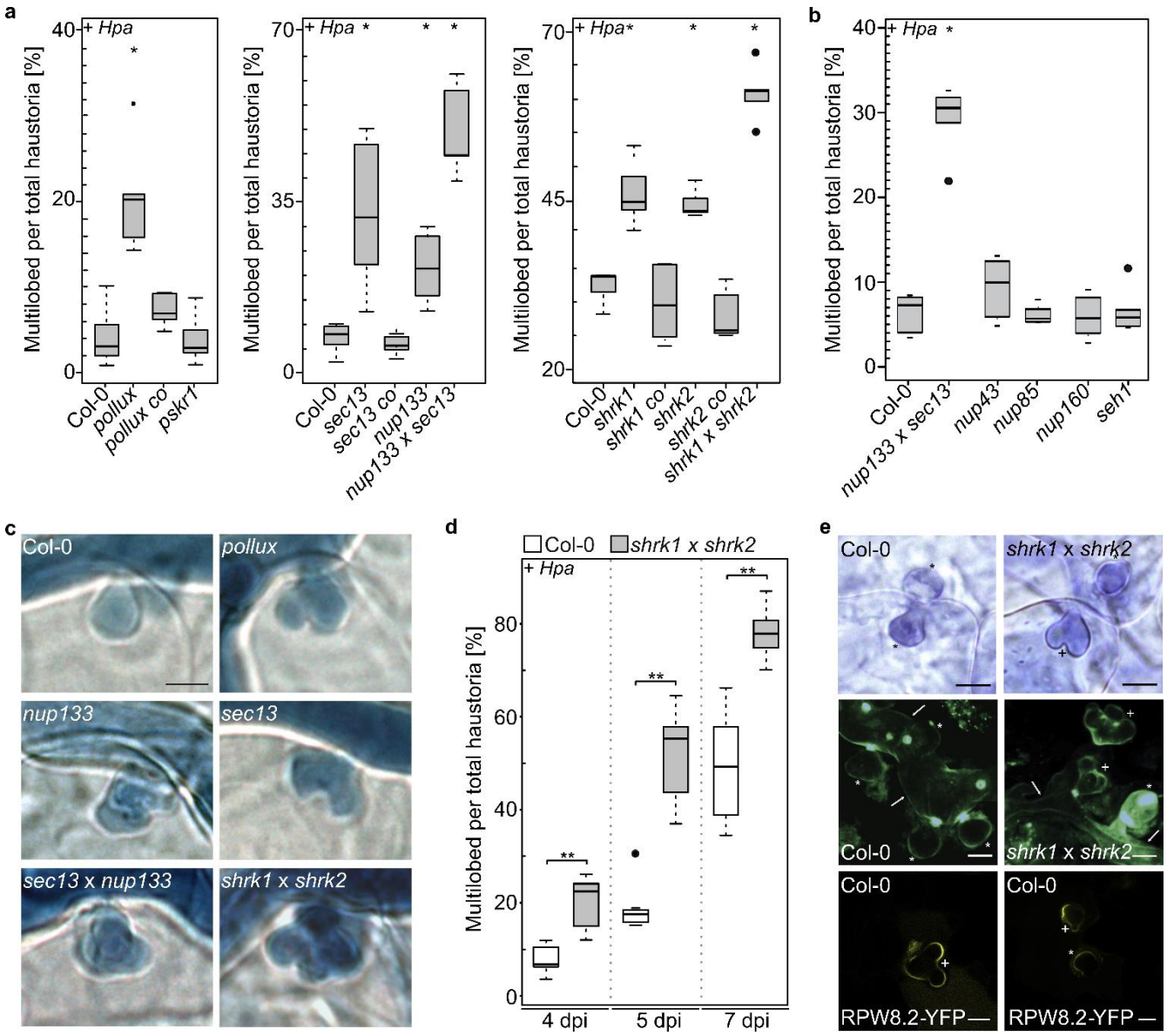

Fig. 2: The morphology of *Hpa* haustoria is altered in *A. thaliana* SNUPO mutants.

Boxplots represent the percentage of multilobed haustoria among total haustoria on *A. thaliana* wild-type (Col-0), the indicated mutants and transgenic homozygous T3 complementation lines (*pollux co, pPOLLUX:POLLUX; sec13 co, pSEC13:SEC13; shrk1 co, pUbi:ShRK1; shrk2 co, pUbi:ShRK2; LjSYMRK, pUbi:Lotus japonicus SYMRK-mOrange*) 5 dpi with *Hpa* isolate NoCo2 **(a + b)**, or 4, 5 and 7 dpi with *Hpa* isolate NoCo2 **(d)**. For each genotype, at least ten independent stretches of hyphae per leaf have been analysed on at least 5 leaves. On average, 1100 haustoria have been analysed per genotype. **(c)** Representative pictures of intracellular haustoria are displayed. Bars = 25 µm. **(e)** Upper

panel: Light microscopy of Technovit section of *A. thaliana* wild-type (Col-0) or the *shrk1 x shrk2* double mutant 7 dpi with *Hpa* isolate NoCo2. Bars, 10 µm. Middle panel: Confocal light scanning microscopy of leaves of *A. thaliana* wild-type (Col-0) or the *shrk1 x shrk2* double mutant stained with aniline-blue 5 dpi with *Hpa* isolate NoCo2. For every haustorium, the entry point can be identified by the formation of the usually bright callose neck. Bars, 25 µm. Lower panel: Confocal light scanning microscopy of leaves of *A. thaliana* wild-type (Col-0) expressing RPW8.2-YFP, which localises to the perihaustorial membrane 7 dpi with *Hpa* isolate NoCo2. *, round haustoria; +, multilobed haustoria; arrows, hyphae. Bars, 10 µm. Black circles, data points outside 1.5 IQR of the upper/lower quartile; bold black line, median; box, Interquartile Range (IQR); whiskers, lowest/highest data point within 1.5 IQR of the lower/upper quartile. Stars indicate significant differences to Col-0 (Wilcoxon-Mann-Whitney test with Bonferroni-Holm correction; *, $p < 0.05$; **, $p < 0.01$; ***, $p < 0.001$). Each experiment was performed at least three times independently.

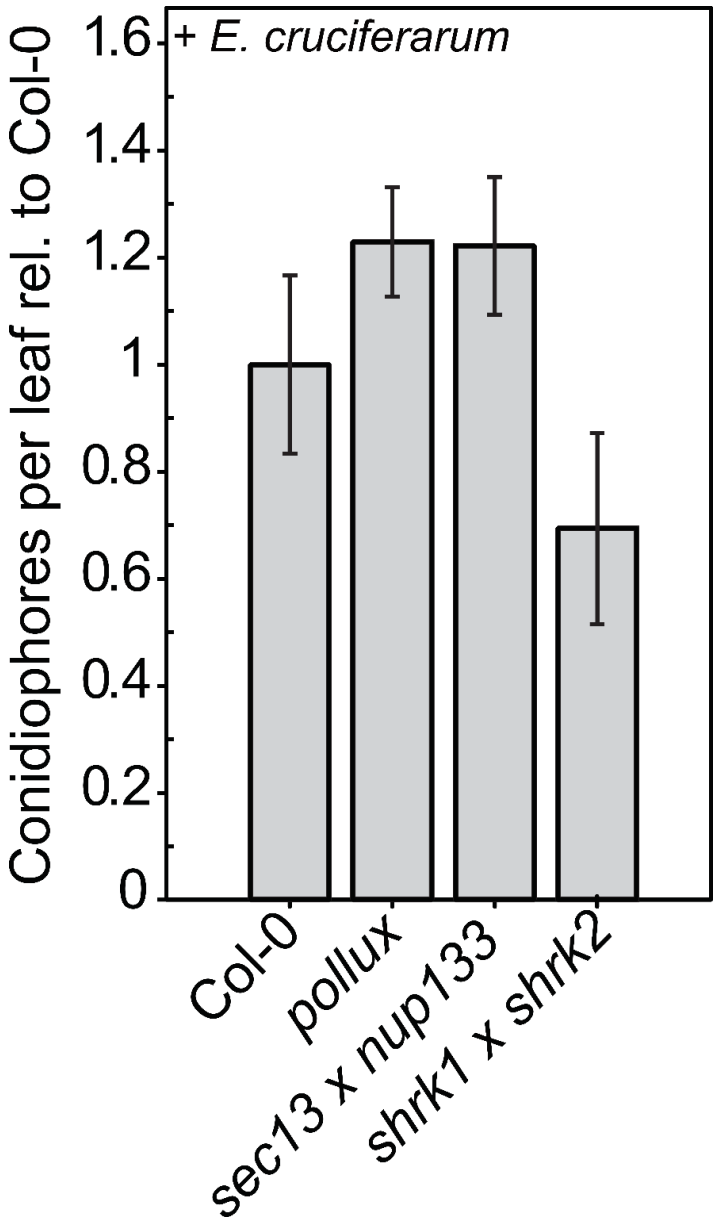

Fig. 3: Mutations in *A. thaliana* SNUPO genes do not impair the reproductive success of the fungal powdery mildew pathogen *E. cruciferarum*.

Bar charts represent the mean number of conidiophores ± s.e.m on leaves of the indicated mutants relative to the wild-type (Col-0) 5 dpi with *E. cruciferarum*. At least ten colonies per leaf on at least 6 leaves have been counted. No significant differences to Col-0 were detected (Wilcoxon-Mann-Whitney test with Bonferroni-Holm correction; *, $p < 0.05$; **, $p < 0.01$; ***, $p < 0.001$).

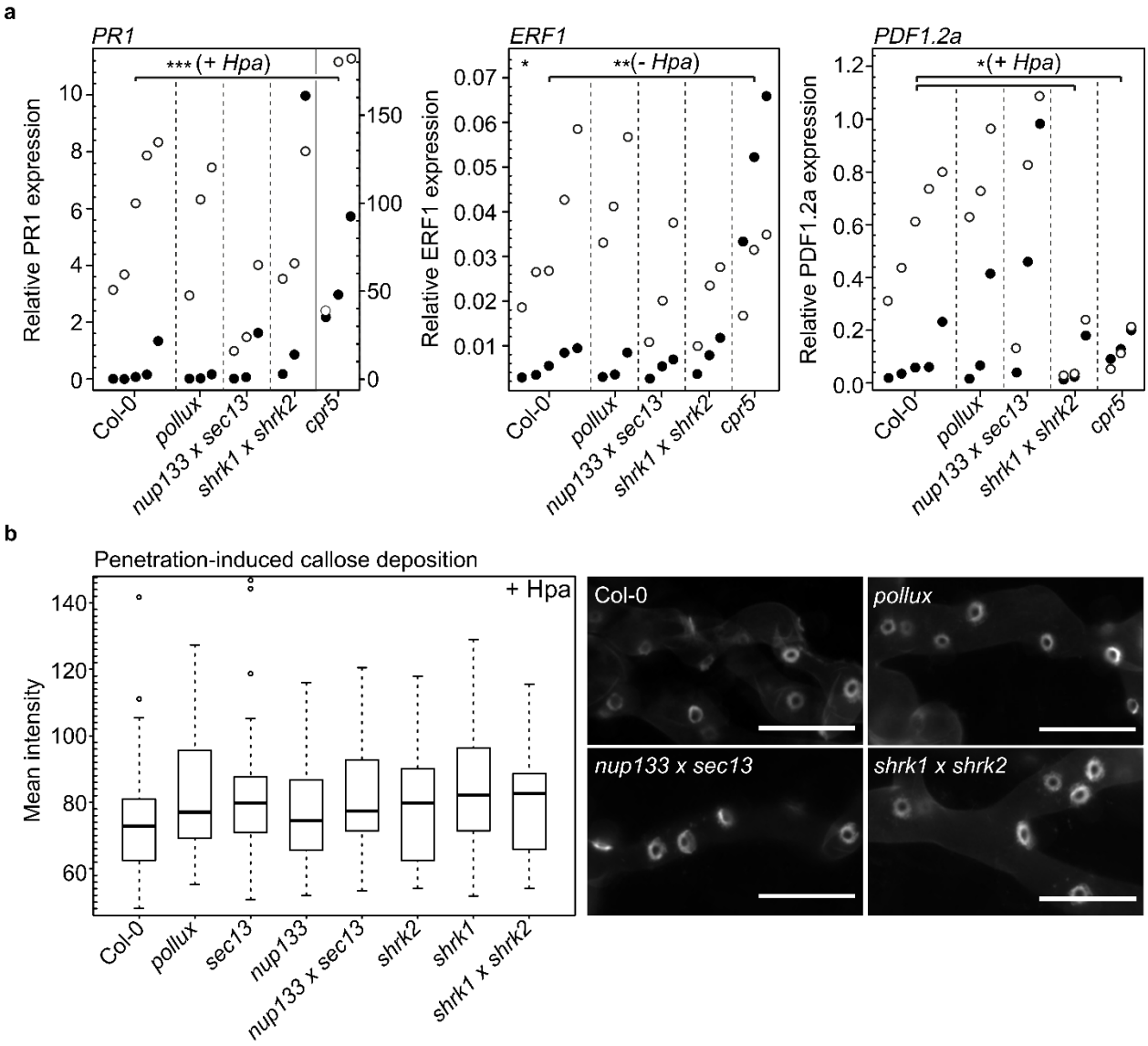

Fig. 4: Activation of defence responses in response to *Hpa* infection is unaltered in *A. thaliana* SNUPO mutants.

(a) Expression of *PR1*, *ERF1* or *PDF1.2a* relative to the housekeeping genes *TIP41-like* and *PP2A* in mock-treated samples (black circles) or in *Hpa*-infected samples (empty circles) was determined in three biological replicates for each genotype by qRT-PCR. Stars indicate significant differences to Col-0 (Dunnett's Test with Bonferroni correction; *, $p < 0.05$). **(b)** Boxplots represent the mean intensity of callose deposition in leaves of *A. thaliana* wild-type (Col-0) or the indicated mutants 4 dpi with *Hpa* isolate NoCo2. n = 27 - 72. Circles, data points outside 1.5 IQR of the upper/lower

quartile; bold black line, median; box, IQR; whiskers, lowest/highest data point within 1.5 IQR of the lower/upper quartile. No significant differences to Col-0 were detected (Wilcoxon-Mann-Whitney test with Bonferroni-Holm correction; *, $p < 0.05$; **, $p < 0.01$; ***, $p < 0.001$). Representative pictures of haustoria-associated callose deposition at the neck band of *Hpa* haustoria growing on the indicated mutants are shown on the right. Bars, 25 µm.

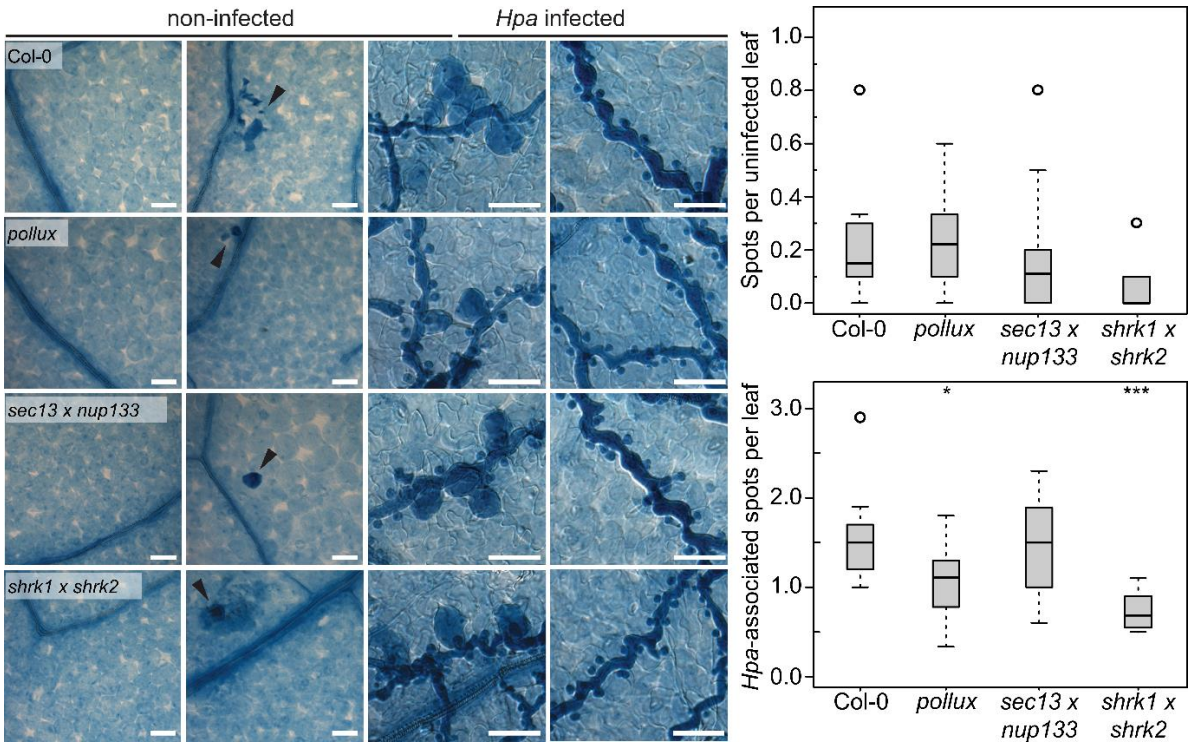

Fig. 5: Cell death responses are unaltered in *A. thaliana* SNUPO mutants.

Differential interference contrast microscopy of *A. thaliana* wild-type (Col-0) and CSG mutant leaves stained with trypan-blue lactophenol 4 dpi with *Hpa* isolate NoCo2. First column, non-infected without cell death; second column, non-infected with random cell death; third column, infected with cell death in, or adjacent to, haustoria-containing cells; fourth column, infected without cell death. Bars, 25 µm**.** Boxplots represent the number of random (upper graph) or *Hpa*-associated (lower graph) cell death spots per leaf on *A. thaliana* wild-type (Col-0) or the indicated mutants 5 dpi with *Hpa* isolate NoCo2. On each leaf four to ten spots have been analysed and a total of five leaves per genotype were investigated. Circles, data points outside 1.5 IQR of the upper/lower quartile; bold black line, median; box, IQR; whiskers, lowest/highest data point within 1.5 IQR of the lower/upper quartile. Stars indicate significant differences to Col-0 (Wilcoxon-Mann-Whitney test with Bonferroni-Holm correction; *, $p < 0.05$; **, $p < 0.01$; ***, $p < 0.001$).

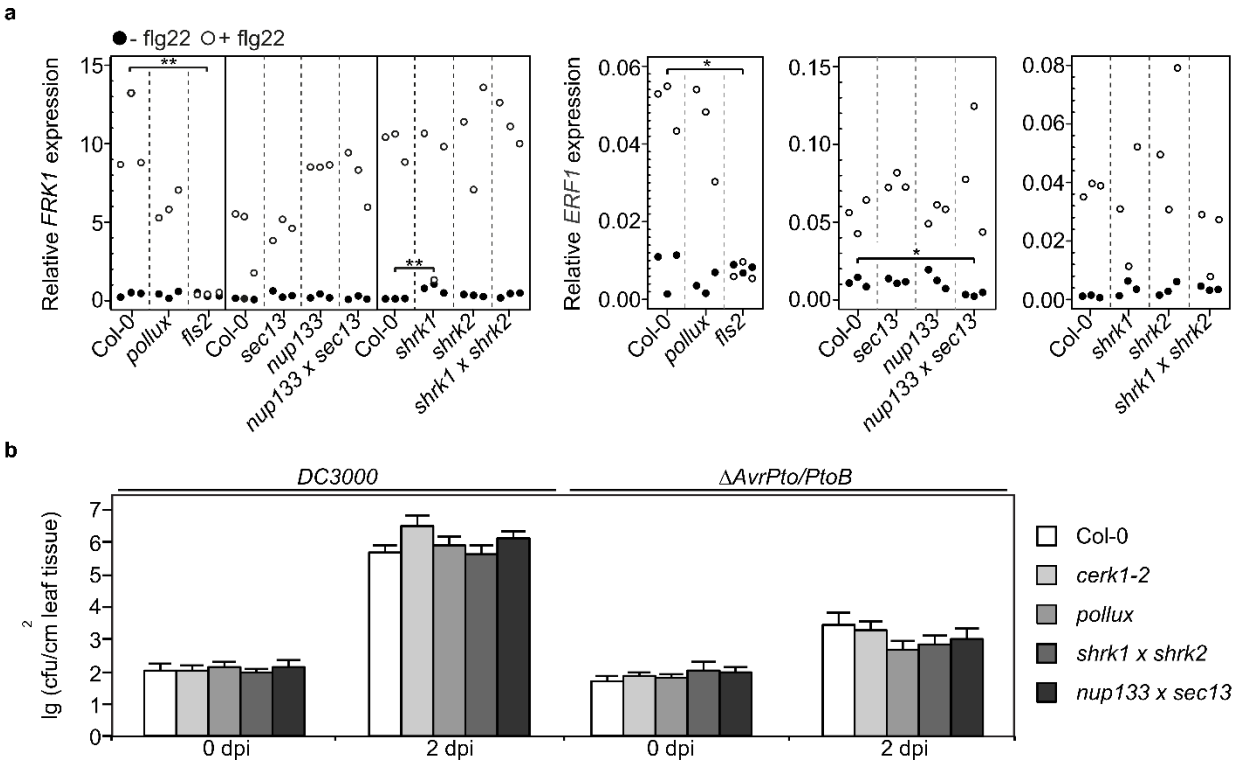

Fig. 6: Expression of flg22-inducible genes as well as growth of the bacterial pathogen *Pseudomonas syringae* are not affected in *A. thaliana* SNUPO mutants.

(a) Expression of *FRK1* and *ERF1* relative to the housekeeping genes *TIP41-like* and *PP2A* in mock-treated samples (black circles) or in flg22-treated samples (empty circles) was determined in three biological replicates for each genotype by qRT-PCR. The *fls2* mutant served as negative control. Stars indicate significant differences to Col-0 (Dunnett's Test with Bonferroni correction; *, $p < 0.01$; **, $p < 0.001$). **(b)** Bacterial density of *Pto* DC3000 or *Pto* DC3000 Δ*AvrPto/PtoB* on *A. thaliana* wild-type (Col-0) or the indicated mutants was determined as colony forming units per cm^2 2 dpi. Data represent means ± s.d. of six replicate measurements/genotype/data point. Results from one representative of at least four independent experiments are shown.

SUPPORTING INFORMATION

```
                    1       10        20        30        40        50        60        70        80        90       100       110       120       130
                    |--------+---------+---------+---------+---------+---------+---------+---------+---------+---------+---------+---------+---------|
At5g49960/AtPOLLUX                                                                  MPIHTPRRTSLFQRSKTLPTNSYRRFTSPYIP----TFRYDD------GDTVSYDGDDSSNL
BAD89022/LjPOLLUX   MIPLPVAAANSNSNSNSNSNDEESPNLSTVIKPPLKKTKTLLPPPSSSSSNRPLHLRVSIDNNNNNNNAPPPPADFSDHQWNYPSFLGTTTRKRRPSSVKPPSTSNLRFDTIPKTKTKTKTNTNTNTNT
Consensus           ............................................................mPihadrrdhqf#rpkfLgTnsrrRrpSpViP....nlR%Dd......gdktnt#g#dnsN1

                    131     140       150       160       170       180       190       200       210       220       230       240       250       260
                    |--------+---------+---------+---------+---------+---------+---------+---------+---------+---------+---------+---------+---------|
At5g49960/AtPOLLUX  PTVPNPEEKPVPVPSQSPSQRITRLWTQFS-LTHCLKFICSCSFTYYMFLRSKVSRLEAENIILLTRCN---SSSDNN----------EMEETNSRAVVFFSVIITFVLPFLLYMYLDLSHVKNLLRRT
BAD89022/LjPOLLUX   NTNTNTDLPPPVPSSSPVARPQHHNHRSPPIFYLLIITCIIFVPYSSYLQYKLAKLEDHKLHLCRQSQIHFSSGHGNGKISIPIHDASFSYILSRKAALYIVLFTLILPFLLYKYLDYLPQIINFLRRT
Consensus           nTnpNp#ekPpPVPSqSPsaRiqrhnhrfp.ifhcLiiiCicffpYsm%LrsKlarLEaenihLcrrc#...SSgdnN..........emeeinSRaaal%iViiTl!LPFLLYkYLDdLpq!iNlLRRT

                    261     270       280       290       300       310       320       330       340       350       360       370       380       390
                    |--------+---------+---------+---------+---------+---------+---------+---------+---------+---------+---------+---------+---------|
At5g49960/AtPOLLUX  NQKKEDVPLKKRLAYSLDVCFSVYPYAKLLALLATVYLIYYGGLALYAVSDCGVDEALWLSWTFVADSGSHADRVGYGARIVSYAISAGGMLIFATMLGLISDAISKMYDSLRKGKSEVLESNHILILG
BAD89022/LjPOLLUX   HNNKEDVPLKKRIAYMLDVFFSIYPYAKLLALLFATLFLIGFGGLALYAVTGGSLAEALWHSWTYVADSGNHAETQGTGQRVVSVSISSGGMLIFAMMLGLVSDAISEKYDSLRKGKCEVIERNHILILG
Consensus           n#nKEDVPLKKRiAYmLDVcFS!YPYAKLLALLlATlfLIg%GGLALYAVsdcglaEALWhSWT%VADSGnHA#rqGtGaR!VSVaISaGGMLIFAmMLGL!SDAISekYDSLRKGKcEViErNHILILG

                    391     400       410       420       430       440       450       460       470       480       490       500       510       520
                    |--------+---------+---------+---------+---------+---------+---------+---------+---------+---------+---------+---------+---------|
At5g49960/AtPOLLUX  WSDKLGSLLKQLAIANKSIGGGVVVVLAERDKEEMETDIAKFEFDLMGTSVICRSGSPLILADLKKVSVSNARAIIVLGSDENADQSDARALRVVLSLTGVKEGWKGHVVVEMCDLDNEPLVKLVGGERI
BAD89022/LjPOLLUX   WSDKLGSLLKQLAIANKSVGGGVIVVLAEKEKEEMEMDITKLEFDFMGTSVICRSGSPLILADLKKVSVSKARAIIVLASDENADQSDARALRVVLSLTGVKEGLRGHVVVEMSDLDNEPLVKLVGGELI
Consensus           WSDKLGSLLKQLAIANKS!GGGV!VVLAEr#KEEMEmDIaKlEFDlMGTSVICRSGSPLILADLKKVSVSnARAIIVLaSDENADQSDARALRVVLSLTGVKEGlrGHVVVEMcDLDNEPLVKLVGGErI

                    521     530       540       550       560       570       580       590       600       610       620       630       640       650
                    |--------+---------+---------+---------+---------+---------+---------+---------+---------+---------+---------+---------+---------|
At5g49960/AtPOLLUX  ETVVAHDVIGRLMIQCALQPGLAQIWEDILGFENAEFYIKKWPQLDGYCFEDVLISFPNAIPCGVKVAADG-KIVLNPSDDYVLKEGDEILVIAEDDDTYAPGSLPEVRMCHFPKMQDPPKYPEKILFCG
BAD89022/LjPOLLUX   ETVVAHDVIGRLMIQCALQPGLAQIWEDILGFENAEFYIKRWPELDGLSFKDILISFPDAIPCGVKVAADGGKIVINPDDSYVMRDGDEVLVIAEDDDTYSPGSLPEVLKGFFPRIPDAPKYPEKILFCG
Consensus           ETVVAHDVIGRLMIQCALQPGLAQIWEDILGFENAEFYIKrWP#LDGlcFeD!LISFP#AIPCGVKVAADG.KIViNPdDdYV$r#GDE!LVIAEDDDTYaPGSLPEVrkchFPriqDaPKYPEKILFCG

                    651     660       670       680       690       700       710       720       730       740       750       760       770       780
                    |--------+---------+---------+---------+---------+---------+---------+---------+---------+---------+---------+---------+---------|
At5g49960/AtPOLLUX  WRRDIDDMIKVLEALLAPGSELWMFNEVPDQEREKKLTDAGLNISKLVNIKLVHRQGNAVIRRHLESLPLETFDSILILAEQSLENSIVHSDSRSLATLLLIRDIQSKRLPYKDAKSSALRISGFPNCCW
BAD89022/LjPOLLUX   WRRDIDDMIMVLEAFLAPGSELWMFNEVPEKEREKKLAAGGLDVFGLENIKLVHREGNAVIRRHLESLPLETFDSILILADESVEDSVAHSDSRSLATLLLIRDIQSRRLPYKDTKSTSLRLSGFSHNSW
Consensus           WRRDIDDMIkVLEAlLAPGSELWMFNEVP#qEREKKLaaaGL#!fgLeNIKLVHR#GNAVIRRHLESLPLETFDSILILA##S1E#S!aHSDSRSLATLLLIRDIQSrRLPYKDaKSsaLRiSGFpnncW

                    781     790       800       810       820       830       840       850       860       870       880       890       900       910
                    |--------+---------+---------+---------+---------+---------+---------+---------+---------+---------+---------+---------+---------|
At5g49960/AtPOLLUX  IRKMQQASDKSIVISEILDSRTKNLVSVSRISDYVLSNELVSMALAMVAEDKQINRVLEALFAEKGNELCIRPAEFYIYDQEEVCFYDIMRAKQRQEIIIGYRLAGMEQAVINPTDKSKLTKWSLDDVF
BAD89022/LjPOLLUX   IREMQQASDKSIIISEILDSRTRNLVSVSRISDYVLSNELVSMALAMVAEDKQINRVLEELFAEQGNEMCIKPAEFYLFDQEELCFYDIMIRGRARQEIIIGYRLANQERRIINPSEKLVARKWSLGDVF
Consensus           IReMQQASDKSI!ISEILDSRTrNLVSVSRISDYVLSNELVSMALAMVAEDKQINRVLeELFAEqGNE$CIrPAEFYi%DQEElCFYDIMrRaRaRQEIIIGYRLAnqErA!INPs#KlkarKWSLdDVF

                    911 917
                    |-----|
At5g49960/AtPOLLUX  VVIASSQ
BAD89022/LjPOLLUX   VVIASGD
Consensus           VVIASg#
```

```
                    1       10        20        30        40        50        60        70        80        90       100       110       120       130
                    |--------+---------+---------+---------+---------+---------+---------+---------+---------+---------+---------+---------+---------|
At1g67720/AtShRK1          MGLCLAQLAVTCLFLVPFVLSQVTEFVSIDCGCSSNYTDPRTGLGWVSDSEIIKQGKPVT-LANTNWNSMQYRRRRDFPTDNKKYCYRLSTKERRRYIVRTTFLYGGL-GSEEAYPKFQLYLD
At2g37050/AtShRK2     MVRISLLLLCLLVSTCLFTSSS--AQAPGFVSLDCGGAEPFTD-ELGLKWSPDNHLI-YGETAN-ISSVNETRTQYTTLRHFPADSRKYCYTLNVTSRNRYLIRATFLYGNFDNSNNVYPKFDISLG
AAM67418/LjSYMRK    MMELPATRILSQAVTCFLCLYIFIGSASATEGFESIACCADLNYTDPLTTLNYTTDYTWFSDKRSCRKIPETELRNRSNENVRLFDIDEGKRCYNLPTIKNGVYLIRGTFPFDSLNSS------FNASIG
Consensus           .........L.la.l..tCL%......sq..gFvSidCg...n%TDp.tgL.w..D...i..g.....i..t#....qy...R.Fp.D..KyCY.L.t..r.rYl!R.TFl%g.l..S...ypkF#.slg

                    131     140       150       160       170       180       190       200       210       220       230       240       250       260
                    |--------+---------+---------+---------+---------+---------+---------+---------+---------+---------+---------+---------+---------|
At1g67720/AtShRK1   ATKWATVTIQEVSRVYYVEELIVRATSSYVDVCVCCAITGSPFMSTLELRPLNLSMYATDY-EDNFFLKVAARVNFGAPNMDALRYPDDPYDRIWESDINKRPNYLVGVAPGTTRINTSKTINTLTREYPP
At2g37050/AtShRK2   ATHWATIVISETYIIETAELVFLASSPTVSVCLSNATTGQPFISTLELRQLSGSMYGSMLSEDRFYLSYAARINFGAESEASVRYPDDPYDRIWESDLQKKPNYLVDVAAGTVRVSTTLPIESRVDDRPP
AAM67418/LjSYMRK    VIQLGAVRSSRLQDLEI-EGVFRATKDYIDFCLLKGEY-YPFISQLELRP-SPEEYLQDF--PTSVLKLISRNNLG-DTKDDIRFPYDQSDRIWKASSISSSAVPLSSNVSNVDLNANVT--------PP
Consensus           aT.wat!.ise....e..El!frAts.y!dvCl..a.tg.PFiStLELRpls.smY..d..ed.f.LkvaaR.NfGa...d..R%PdDpyDRIWesd..k.pnylv.va.gtvr.nt..ti.......PP

                    261     270       280       290       300       310       320       330       340       350       360       370       380       390
                    |--------+---------+---------+---------+---------+---------+---------+---------+---------+---------+---------+---------+---------|
At1g67720/AtShRK1   MKVMQTAVVGTQGLISYRLNLEDFPANARAYAYFAEIEELGANETRKFKLVQPYFPDYSNAVVNIAENANGSYTLYEPSYMNVTLDFVLTFSFGKTKDSTQGPLLNAIEISKYLPISVKTDRSDVSVLDA
At2g37050/AtShRK2   QKVMQTAVVGTNGSLTYRMNLDGFPGFGWAFTYFAEIEDLAEDESRKFRLVLPEQPEYSKSVVNIKENTQRPYRVYAPGYPNITLPFVLNFRFAKTADSSRGPLLNAMEISKYLRKS--DGSVDATVMAN
AAM67418/LjSYMRK    LTVLQTALTDPERLEFIHTDLETEDYGYRVFLYFLELDRTLQAGQRVFDIYV--NSEIKKESFDVLAGGSN----YRYDVLDISASGSLNVTLVKASKSEFGPLLNAYEILQVRPWIEETNQTDVGVIQK
Consensus           .kV$QTAvvgt#gl..yr.#L#.fp...ra%.YFaEi#.l...e.RkF.lv.p..p#ysk.vv#!.en....y..Y.p.y.#!tl.fvLnf.f.Kt.dS..GPlLNA.EIskylp.s..t...Dv.V...

                    391     400       410       420       430       440       450       460       470       480       490       500       510       520
                    |--------+---------+---------+---------+---------+---------+---------+---------+---------+---------+---------+---------+---------|
At1g67720/AtShRK1   IRS---MSPDSDWASEG--GDPCIPVLWSWVNCS-STSPPRVTKIALSRKNLRGEIPPGINYMEALTELWLDDNELTGTLPDMSKLVNLKIMHLENNQLSGSLPPYLAHLPNLQELSIENNSFKGKIPSA
At2g37050/AtShRK2   VAS---LYSSTEWAQEG--GDPCSPSPWSWVQCN-SDPQPRVVAIKLSSNNLTGNIPSDLVKLTGLYELWLDGNSFTGPIPDFSRCPNLEIIHLENNRLTGKIPSSLTKLPNLKELYLQNNVLTGTIPSD
AAM67418/LjSYMRK    MREELLLQNSGNRALESWSGDPCILLPWKGIACDGSNGSSVITKLDLSSSNLKGLIPSSIAEMTNLETLNISHNSFDGSVPSFPLSSLLISVDLSYNDLMGKLPESIVKLPHLKSLYFGCNEHMSPEDPA
Consensus           .rs...$..s.#wA.Eg..GDPCip.pWsw!.C..S...pr!tki.LSs.NL.G.IPs.i..$t.L.eLwld.NsftG..Pdfs...nL.i.hLenN.L.GklP.sl.kLPnLkeLy..nN...g.ipsa

                    521     530       540       550       560       570       580       590       600       610       620       630       640       650
                    |--------+---------+---------+---------+---------+---------+---------+---------+---------+---------+---------+---------+---------|
At1g67720/AtShRK1   LLKGKVLFKYNNNPELQNEAQR-KHFWQTLGISIAAVAILLLLVGGSLVLLCALRKTKRADKGDSTETKKKGLYAYSAVRG--GHLLDEGVAYFISLPVLEEATDNFSKKVGRGSFGSVYYGRMKDGKEV
At2g37050/AtShRK2   LAKD-VISNFSGNLNLEKSGDGKGKKLGVIIGASVGAFVLLIATII-SCIVMCKSKKNNKLGKTSELTNRPLPIQRVSSTLS--EAHGD--AAHCFTLYEIEEATKKFEKRIGSGGFGIVYYGKTREGKEI
AAM67418/LjSYMRK    NMNSSLI-----NTDYGRCKGKESRFGQVIVIGAITCGSLLITLAFGVLFVCRYRQKLIPWEGFAGKKYPMETNIIFSLPSKDDFFIKSVSIQAFTLEYIEVATERYKTLIGEGGFGSVYRGTLNDGQEV
Consensus           l.k..vi.....N.#l.....k.k.fgq!igis..a...Ll.t...s....C..rk.....kg......p......ss..s......d...a..ftL..iEeAT..%.k.!G.GgFGsVYyG...#GkE!

                    651     660       670       680       690       700       710       720       730       740       750       760       770       780
                    |--------+---------+---------+---------+---------+---------+---------+---------+---------+---------+---------+---------+---------|
At1g67720/AtShRK1   AVKITADPSSHLNRQFVTEVALLSRIHHRNLVPLIGYCEEADRRILVYEYMHNGSLGDHLHGSSDY-KPLDWLTRLQIAQDAAKGLEYLHTGCNPSIIHRDVKSSNILLDINMRAKVSDFGLSRQT-EED
At2g37050/AtShRK2   AVKVLANNSYQGKREFANEVTLLSRIHHRNLVQFLGYCQEEGKNMLVYEFMNNGTLKEHLYGVVPRDRRISWIKRLEIAEDAARGIEYLHTGCVPAIIHRDLKTSNILLDKHMRAKVSDFGLSKFA-VDG
AAM67418/LjSYMRK    AVKVRSATSTQGTREFDNELNLLSAIQHENLVPLLGYCNESDQQILVYPFMSNGSLQDRLYGEPAKRKILDWPTRLSIALGAARGLAYLHTFPGRSVIHRDIKSSNILLDHSMCAKVADFGFSKYAPQEG
Consensus           AVK!.a..S.qg.R#F.nEv.LLSrIhHrNLVpllGYC#E.d..iLVYe%MhNGsL.#hLyG.....k.ldW.tRL.IA.dAArGleYLHTgc.ps!IHRD.KsSNILLD..MrAKVsDFGlSk.a..#g

                    781     790       800       810       820       830       840       850       860       870       880       890       900       910
                    |--------+---------+---------+---------+---------+---------+---------+---------+---------+---------+---------+---------+---------|
At1g67720/AtShRK1   LTHVSSVAKGTVGYLDPEYYASQQLTEKSDVYSFGVVLFELLSGKKPVSAEDFGPEL-NIVHWARSLIRKGDVCGIIDPCIASN-VKIESVWRVAEVANQCVEQRGHNRPRMQEVIVAIQDAIRIEREGNE
At2g37050/AtShRK2   TSHVSSIVRGTVGYLDPEYYISQQLTEKSDVYSFGVILLELMSGQEAISNESFGVNCRNIVQWAKMHIDNGDIRGIIDPALAEDDYSLQSMWKIAEKALLCVKPHGNMRPSMSEVQKDIQDAIRIEKEAL
AAM67418/LjSYMRK    DSYVSLEVRGTAGYLDPEYYKTQQLSEKSDVFSFGVVLLEIVSGREPLNIKRPRTEW-SLVEWATPYIRGSKVDEIYDPGIKGG-YHAEAMWRVVEVALQCLEPFSTYRPSMVAIVRELEDALIIENNAS
Consensus           .shVSs.vrGTvGYLDPEYY.sQQLtEKSDV%SFGV!LlEl.SG.ep.s.e.fg.#..niV.WA...Ir.gd!.gI!DP.ia...y..#smWr!aEvAlqCvep.g..RPsM.e!...i#DAirIE..a.

                    911     920       930       940       950   956
                    |--------+---------+---------+---------+-----|
At1g67720/AtShRK1   NGLKSSSSSSSKAQSSRKTLLTSFLELESPD----ISRNSLAPAAR
At2g37050/AtShRK2   AARGGISDEFSRSSAHSSSLNMGHLDLAGSQSYVSIDESVLQPTAR
AAM67418/LjSYMRK    EYMKSIDSLGGSNRYSIVIEKRVLPSTTSTAESTITTQSLSHPQPR
Consensus           ...ksiss..s....s...l....l.l.s......i..s.l.P.aR
```

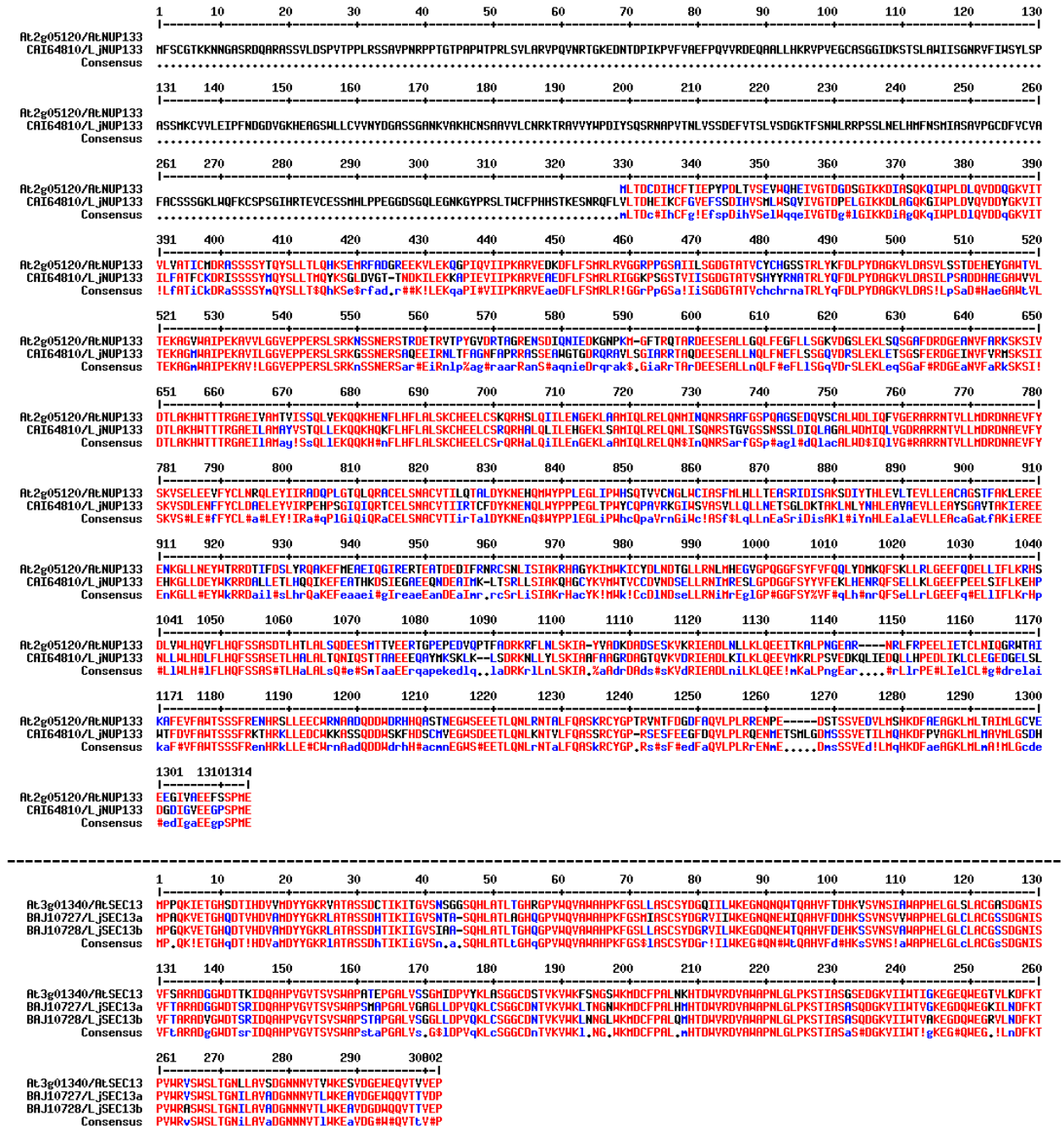

S1 Fig. Alignments of the protein sequences of *L. japonicus* CSGs and closely related *A. thaliana* SNUPO genes.

TAIR/GenBank protein identifiers are shown. Red, consensus level high = 90%; blue, consensus level low = 50%. Alignments were generated using the multiple sequence alignment software by Corpet (Corpet, 1988).

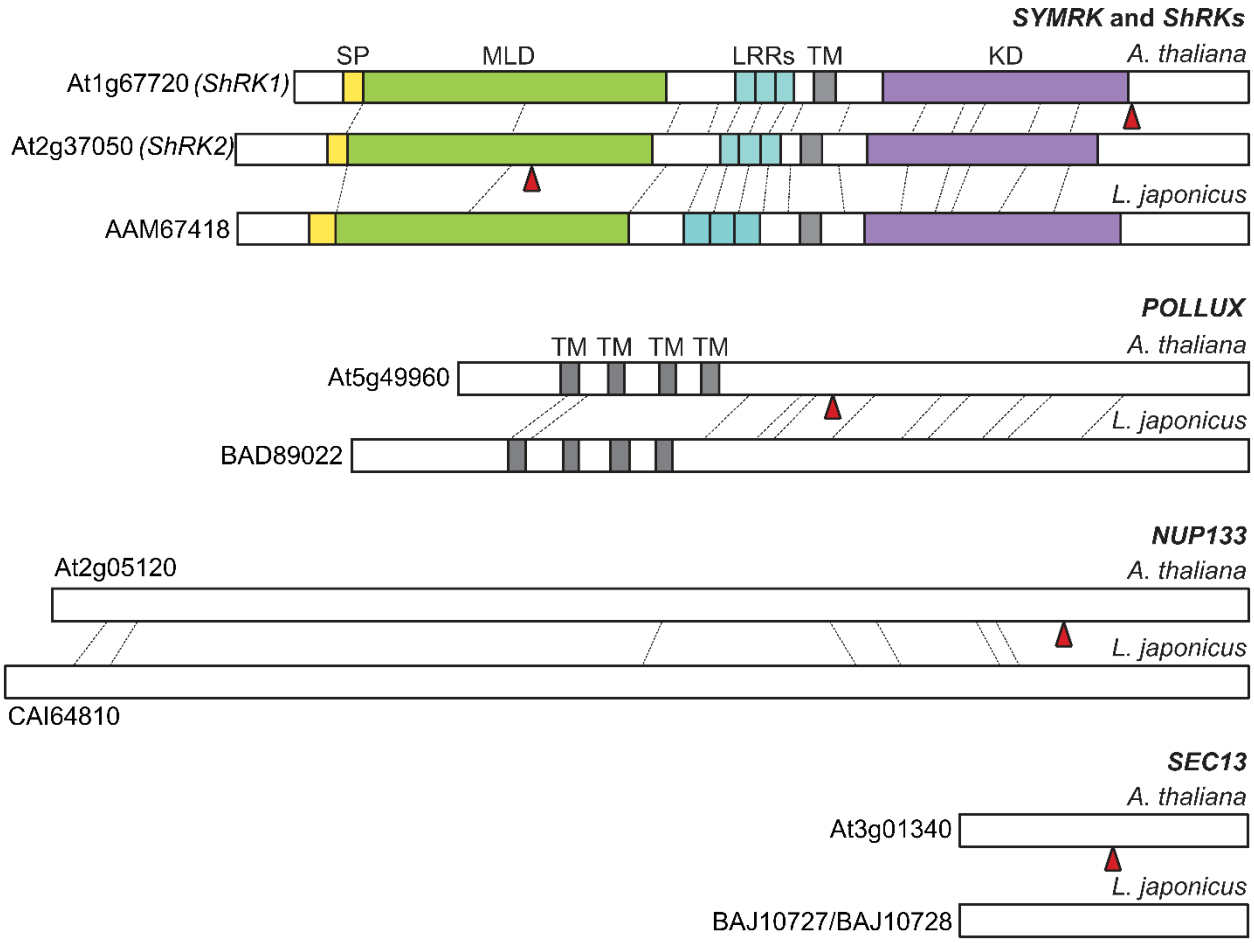

S2 Fig. Comparison of gene structures and protein domains of *L. japonicus* CSGs and closely related *A. thaliana* SNUPO genes.

TAIR/GenBank protein identifiers are shown; dashed lines, positions of introns in the original gene sequence; red triangles, positions of T-DNA insertion in the respective mutants; SP, signal peptide; MLD, malectin-like domain; LRRs, leucine-rich repeats; TM, transmembrane domain; KD, kinase domain.

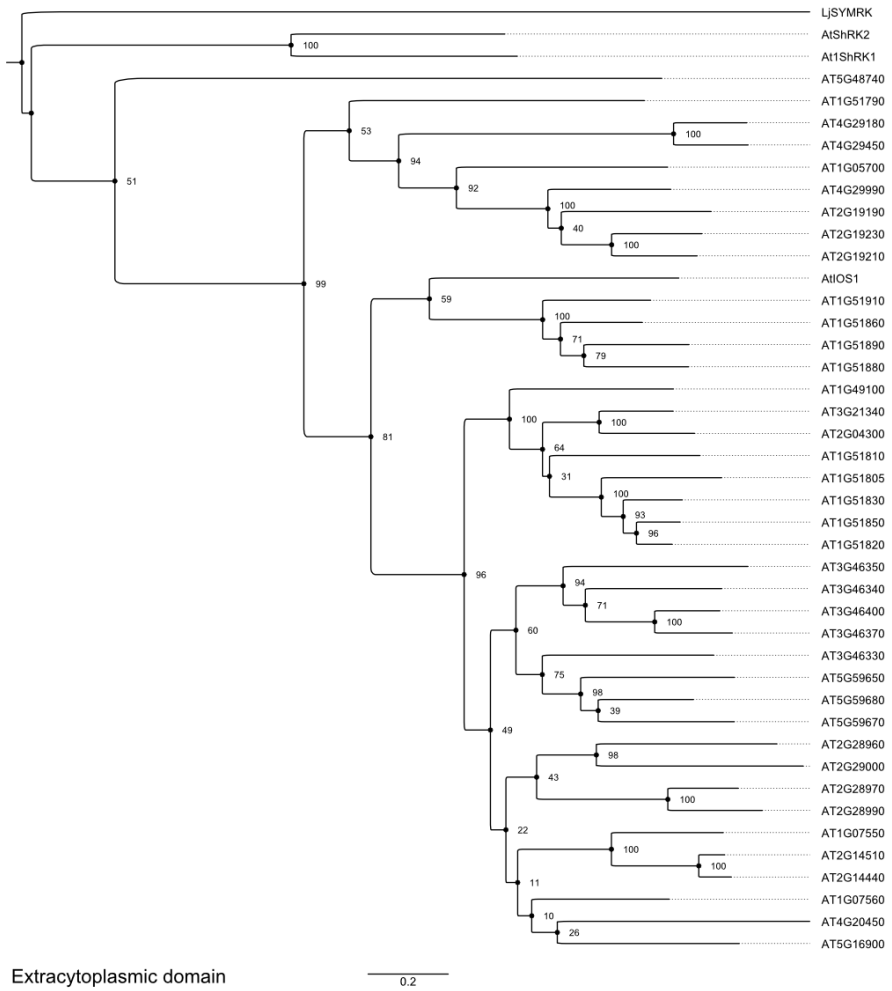

S3 Fig. Maximum likelihood phylogenetic tree of the extracytoplasmic domains of MLD-LRR-RKs from *A. thaliana* and *L. japonicus* SYMRK.

The specific domain composition featuring a MLD followed by the conserved gly-asp-pro-cys (GDPC) motif known to be required for the proper establishment of the symbiotic program in the root epidermis (Kosuta *et al.*, 2011; Antolín-Llovera *et al.*, 2014), and LRRs is not restricted to SYMRK but can also be found in 42 of the 50 members of LRR I-RLKs present in *A. thaliana* (Shiu & Bleecker, 2003; Hok *et al.*, 2011). A maximum likelihood phylogenetic tree based on the extracytoplasmic regions (excluding the signal peptides) of 42 MLD-LRR-RK proteins from *A. thaliana* and SYMRK from *L. japonicus*. Numbers on each node represent the respective bootstrap values. Bar, relative genetic distance (arbitrary unit).

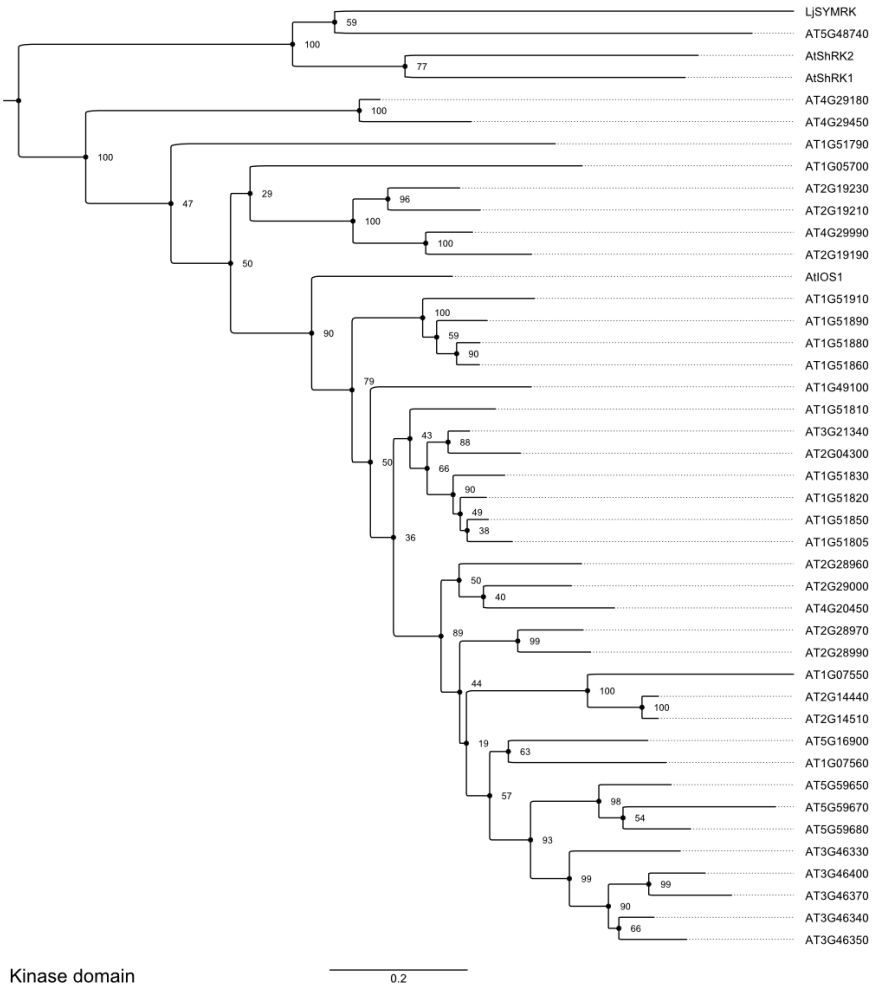

S4 Fig. Maximum likelihood phylogenetic tree of the highly conserved kinase domains of MLD-LRR-RKs from *A. thaliana* and *L. japonicus* SYMRK.

A maximum likelihood phylogenetic tree based on the highly conserved kinase domains of 42 MLD-LRR-RK proteins from *A. thaliana* and SYMRK from *L. japonicus*. Numbers on each node represent the respective bootstrap values. Bar, relative genetic distance (arbitrary unit).

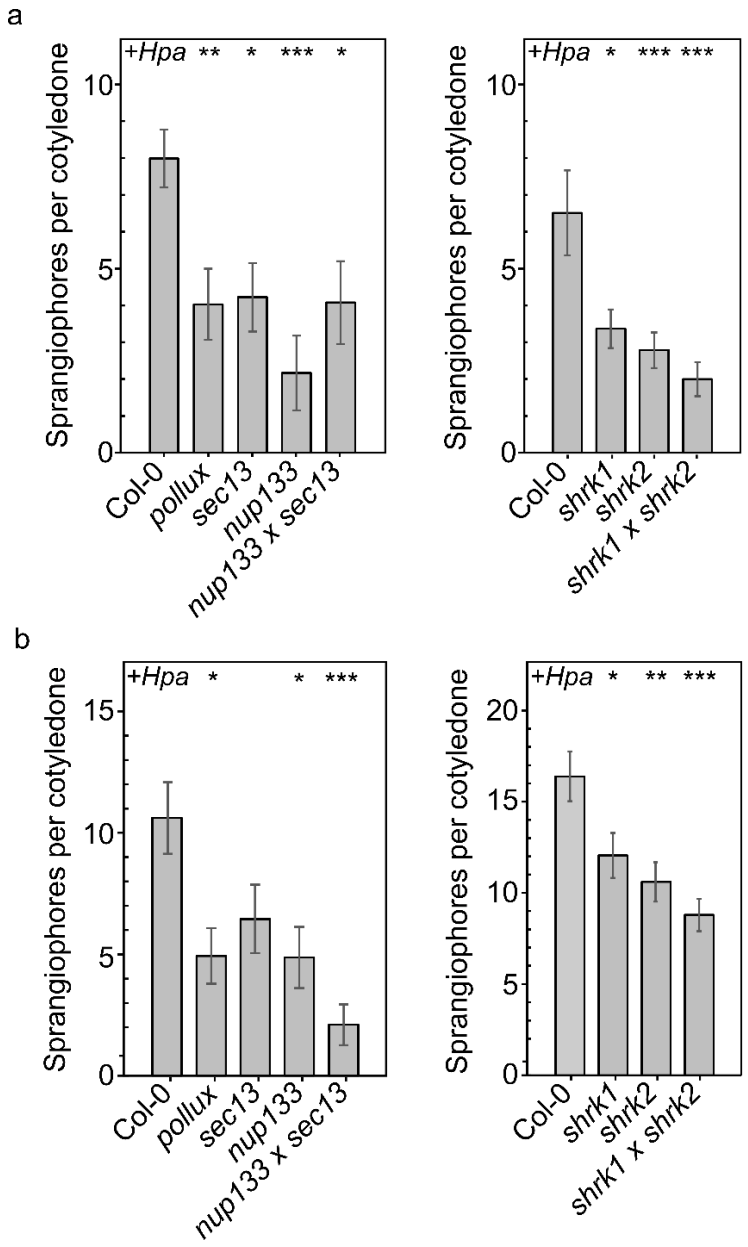

S5 Fig. Mutations in *A. thaliana* SNUPO genes reduce the reproductive success of the oomycete downy mildew pathogen *H. arabidopsidis.*

Bar charts represent the mean number of sporangiophores ± s.e.m on infected cotyledons of *A. thaliana* wild-type (Col-0) or the indicated mutants 4 dpi with *Hpa* isolate NoCo2 in two additional replicates **(a + b)**. n = 21 – 99. Stars indicate significant differences to Col-0 (Wilcoxon–Mann–Whitney test with Bonferroni-Holm correction; *, $p < 0.05$; **, $p < 0.01$; ***, $p < 0.001$).

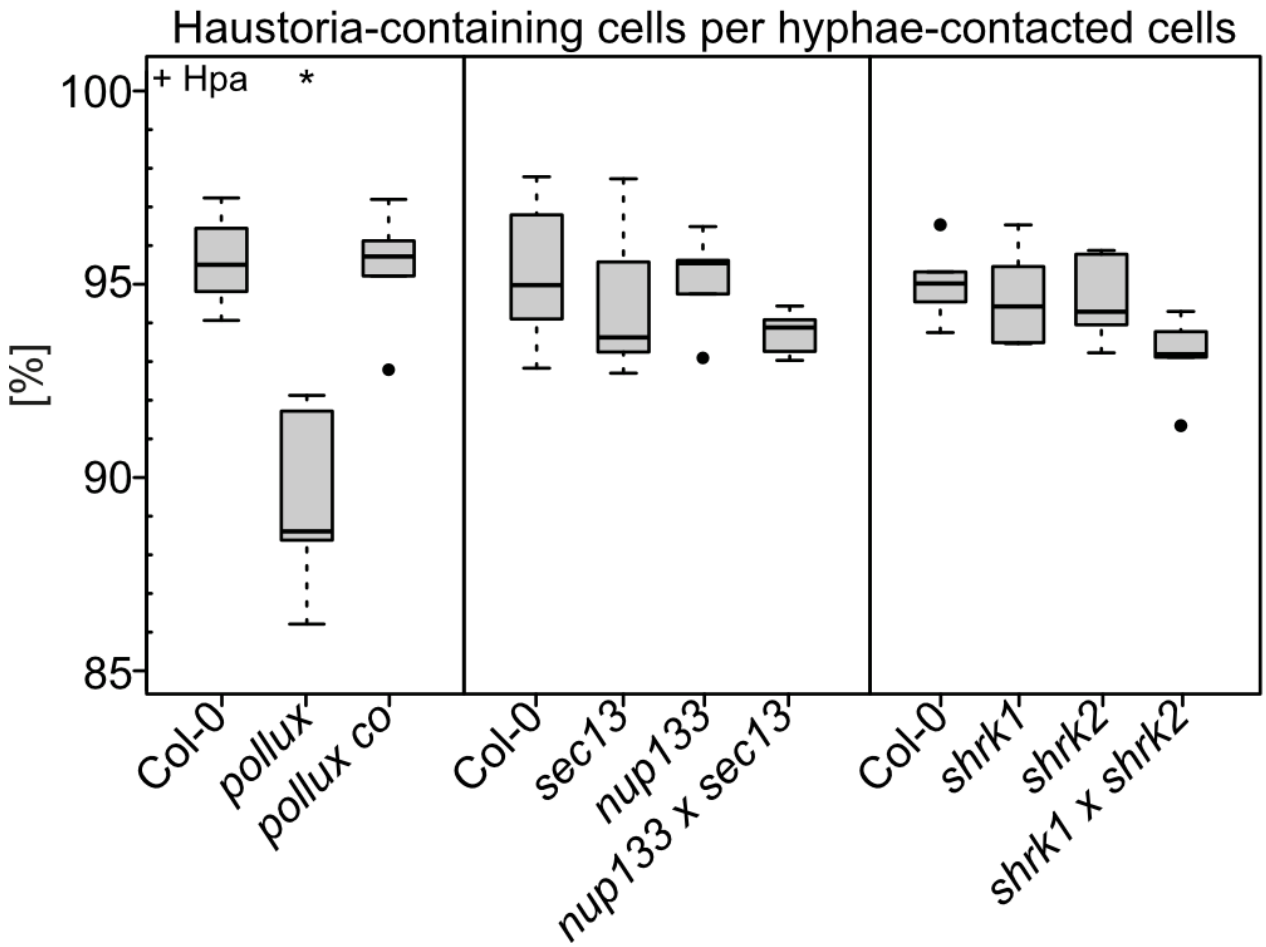

S6 Fig. Mutations in *A. thaliana* SNUPO genes do not reduce the number of cells that accommodate haustoria.

Boxplots represent the percentage of haustoria-containing cells per cells contacted by hyphae on leaves of *A. thaliana* wild-type (Col-0), the indicated mutants and the transgenic complementation lines (*pollux co*, *pPOLLUX:POLLUX*) 5 dpi with *Hpa* isolate NoCo2. For each genotype, at least ten independent stretches of hyphae per leaf have been analysed on at least 5 leaves. Black circles, data points outside 1.5 IQR of the upper/lower quartile; bold black line, median; box, IQR; whiskers, lowest/highest data point within 1.5 IQR of the lower/upper quartile. Stars indicate significant differences to Col-0 (Wilcoxon–Mann–Whitney test with Bonferroni-Holm correction; *, $p < 0.05$).

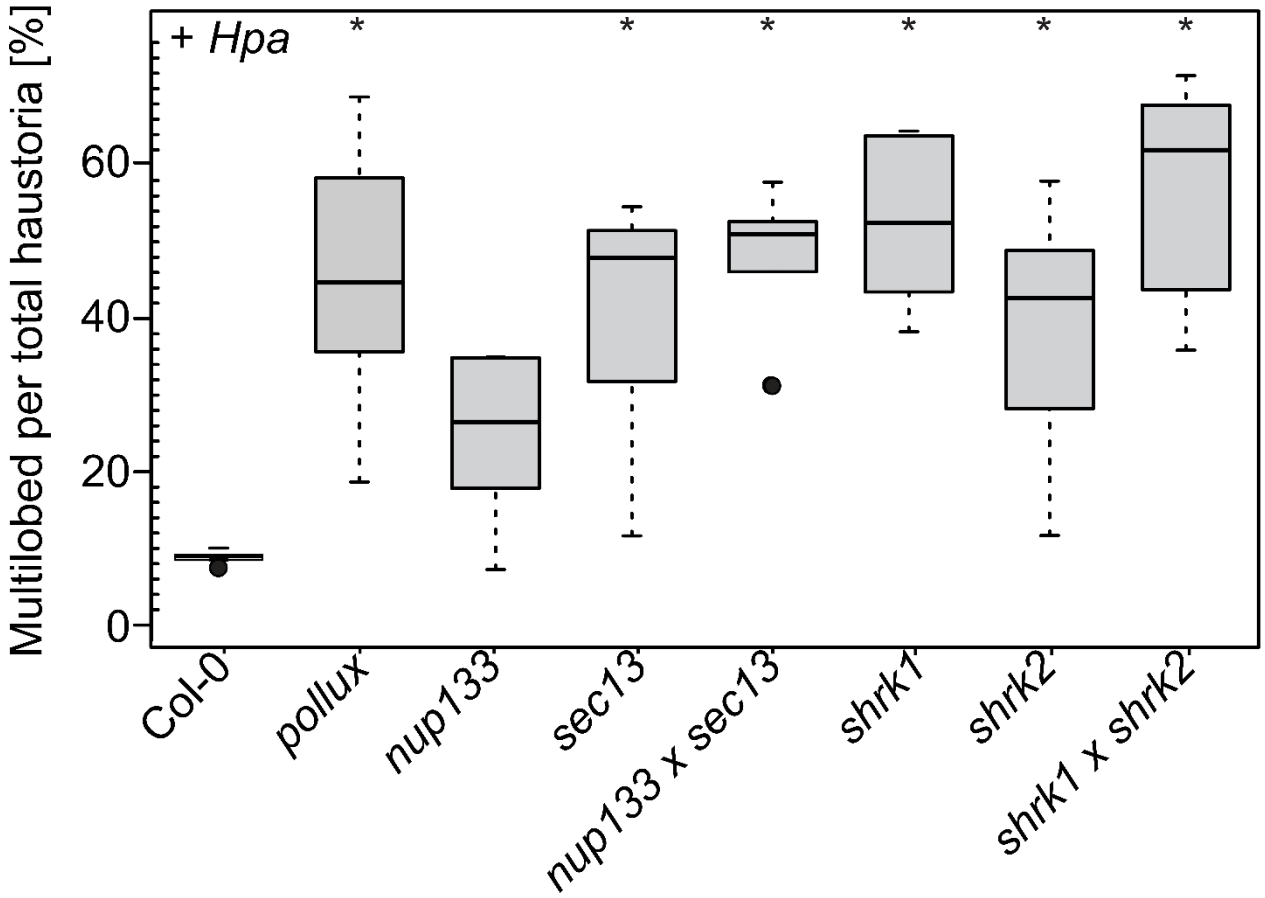

S7 Fig. The morphology of *Hpa* haustoria is altered in *A. thaliana* SNUPO mutants.

Boxplots represent the percentage of multilobed haustoria among total haustoria on *A. thaliana* wild-type (Col-0) or the indicated mutants 5 dpi with *Hpa* isolate NoCo2. For each genotype, at least ten independent stretches of hyphae per leaf have been analysed on at least 5 leaves. On average, 1100 haustoria have been analysed per genotype. Black circles, data points outside 1.5 IQR of the upper/lower quartile; bold black line, median; box, IQR; whiskers, lowest/highest data point within 1.5 IQR of the lower/upper quartile. Stars indicate significant differences to Col-0 (Wilcoxon–Mann–Whitney test with Bonferroni-Holm correction; *, $p < 0.05$).

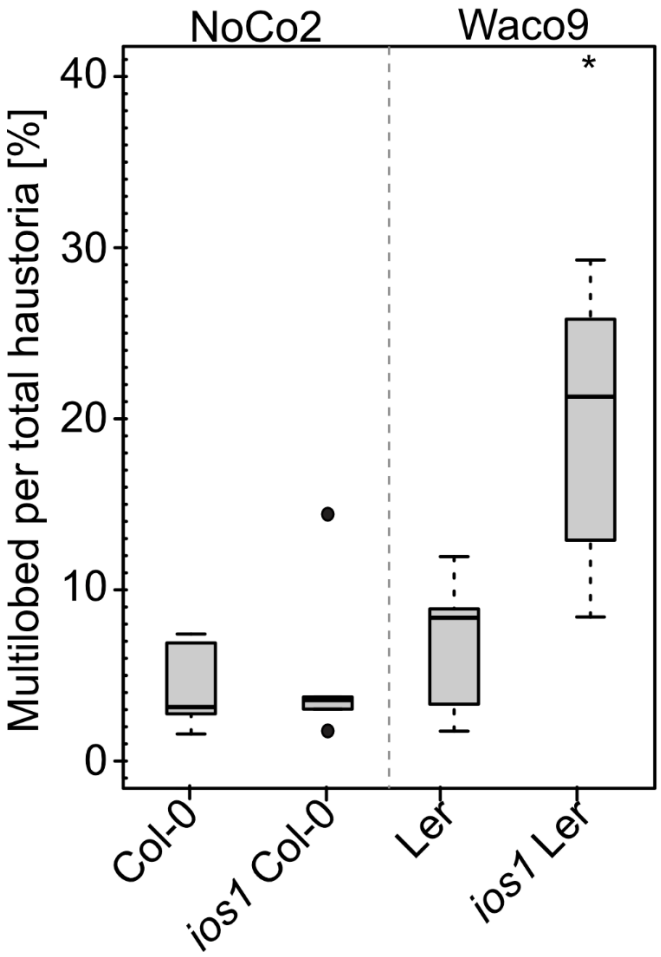

S8 Fig. An increased frequency of multilobed *Hpa* haustoria in a *A. thaliana ios1* mutant was observed in the Ler background infected with Waco9, but not in the Col-0 background infected with NoCo2.

Boxplots represent the percentage of multilobed haustoria among total haustoria on *A. thaliana* wild-type (Col-0; Ler), and *ios1* mutant lines 5 dpi with *Hpa* isolate NoCo2 (a), 5 dpi with *Hpa* isolate NoCo2 and Waco9. For each genotype, at least ten independent stretches of hyphae per leaf have been analysed on at least 5 leaves. Black circles, data points outside 1.5 IQR of the upper/lower quartile; bold black line, median; box, IQR; whiskers, lowest/highest data point within 1.5 IQR of the lower/upper quartile. Stars indicate significant differences to Col-0 (Wilcoxon–Mann–Whitney test with Bonferroni-Holm correction; *, $p < 0.05$).

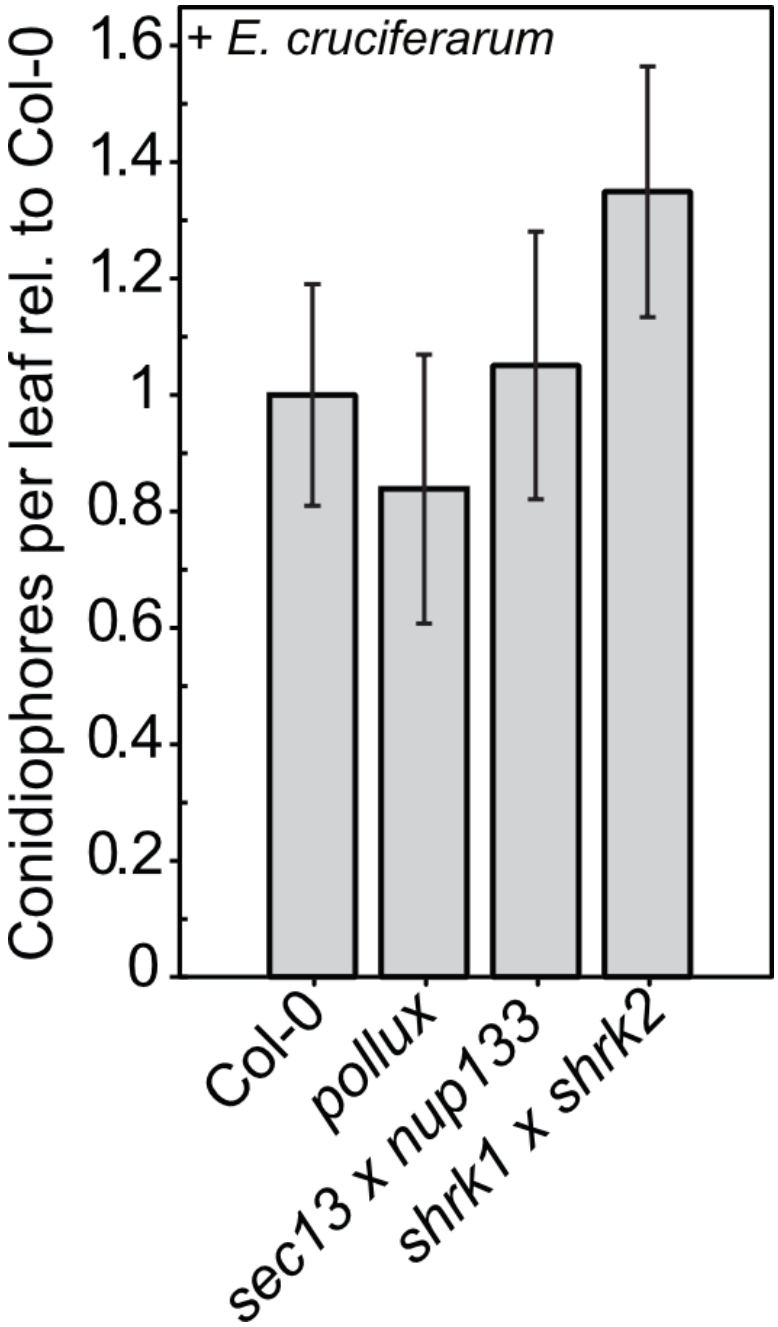

S9 Fig. Mutations in *A. thaliana* SNUPO genes do not impair the reproductive success of the fungal powdery mildew pathogen *E. cruciferarum*.

Bar charts represent the mean number of conidiophores ± s.e.m on leaves of the indicated mutants relative to the wild-type (Col-0) 5 dpi with *E. cruciferarum*. At least ten colonies per leaf on at least 6 leaves have been counted. No significant differences to Col-0 were detected.

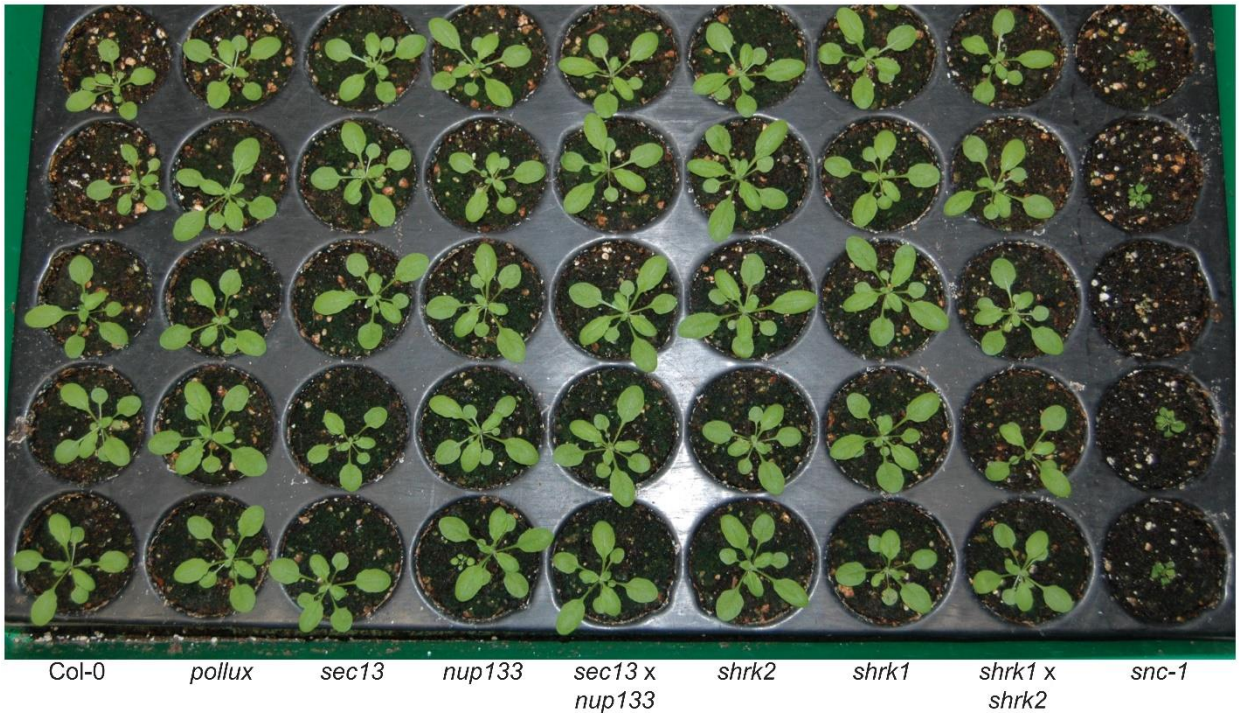

S10 Fig. *A. thaliana* SNUPO mutants do not show developmental or growth defects.

3-week-old *A. thaliana* wild-type (Col-0) plants grown alongside the indicated mutant lines under long day conditions. The dwarf phenotype of *snc1* is included on the far right for comparison.

S1 Table *A. thaliana* SNUPO genes with encoded proteins and their respective identities / similarities to related *L. japonicus* genes.

Sequence identifiers and identities / similarities shared between the protein sequences of *A. thaliana* SNUPO and other nucleoporin genes and those of their respective *L. japonicus* counterparts. The numbers for AtSEC13 indicate the identity / similarity of its amino acid sequence to each of the two predicted LjSEC13 proteins. For ShRK1 and ShRK2, numbers in brackets refer to their kinase domain (KD) only. n.d., not detected. NASC ID: insertion mutant identifier.

Gene	*L. japonicus* homolog (NCBI mRNA/protein IDs)	Gene ID	NASC ID	Protein Identity / Similarity To *L. japonicus*
POLLUX	AB162158 / BAD89022	At5g49960	N566135	71 / 82
SEC13	AB506697 / BAJ10727 - AB506698 / BAJ10728	At3g01340	N662322	80-82 / 92-91
NUP133	AJ890251 / CAI64810	At2g05120	N565761	55 / 71
SEH1	AB506696 / BAJ10726	At1g64350	N653094	64 / 78
NUP43	n.d.	At4g30840	N803490	n.d.
NUP85	AB284835 / BAF45348	At4g32910	N613274	61 / 75
NUP160	n.d.	At1g33410	N624418	n.d.
ShRK1	(*SYMRK*) AF492655 / AAM67418	At1g67720	N467036	33 (48KD) / 49 (68KD)
ShRK2		At2g37050	N643700	34 (48KD) / 50 (68KD)

S2 Table Constructs and cloning strategy.

Constructs labelled with "GG" were generated via Golden Gate cloning. For details on assembly method, general modules and plasmids (Gxx, BBxx), see (Binder *et al.*, 2014). Golden Gate constructs contain silent mutations to facilitate cloning.

Entry clones / Golden Gate Level I & Level II plasmids (LI & LII)

Name	**Description**
pENTR-pSEC13:SEC13	Phusion PCR product consisting of *SEC13* genomic construct amplified from *A. thaliana* gDNA with sec13co_FW and sec13co_RV, cloned into *pENTR/D-TOPO* (Invitrogen) via TOPO reaction.
LI A-C *pPOLLUX* (GG)	LI promoter element of *POLLUX* (1523 bp). Assembled from 2 PCR fragments amplified from *A. thaliana* gDNA by BpiI cut ligation into LI-BpiI vector. Fragment 1: AtPol-Pro1+ & AtPol-Pro2- Fragment 2: AtPol-Pro3+ & AtPol-Pro4-
LI C-D *POLLUX* (GG)	LI element containing genomic *POLLUX*. Assembled from 2 PCR fragments amplified from *A. thaliana* gDNA by BpiI cut ligation into LI-BpiI vector. Fragment 1: AtPol1+ & AtPol2- Fragment 2: AtPol3+ & AtPol4-
LII F 1-2 *pPOLLUX:POLLUX* (GG)	Assembled by BsaI cut ligation from: LI A-C *pPOLLUX* + LI C-D *POLLUX* + LI dy D-E (BB8) + LI E-F *35S-T* (G59) + LI F-G neo (G3) + LIIc F1-2 (BB30)
LII R 3-4 *p35S:mCherry* (GG)	Assembled by BsaI cut ligation from: LI A-B *p35S* (G5) + LI dy B-C (BB6) + LI C-D *mCherry* (G23) + LI dy D-E (BB8) + LI E-F *nos-T* (G6) + LI dy F-G (G9) + LIIc R 3-4 (BB33)
LII R 5-6 *p35S:mCherry* (GG)	Assembled by BsaI cut ligation from:

	LI A-B *p35S* (G5) + LI dy B-C (BB6) + LI C-D *mCherry* (G23) + LI dy D-E (BB8) + LI E-F *HSP-T* (G45) + LI dy F-G (G9) + LIIc R 5-6 (BB37)
LI A-C *ShRK1* (GG)	Full length genomic DNA from ATG to codon prior to STOP (bases 1-4360); silent mutations introduced to remove type IIS restriction sites; obtained by gene synthesis (GenScript)
LI A-C *ShRK2* (GG)	Full length genomic DNA from ATG to codon prior to STOP (bases 1-4185); silent mutations introduced to remove type IIS restriction sites; obtained by gene synthesis (GenScript)
LII F 1-2 *pUBi: ShRK1-YFP* (GG)	Assembled by BsaI cut ligation from: LI A-B *pUBi* (G7) + LI dy B-C (G4) + LI A-C *ShRK1* + LI D-E *YFP* (G12) + LI E-F *35S-T* (G59) + LI F-G hygro (G94) + LIIc F 1-2 (BB30)
LII F 1-2 *pUBi: ShRK2-YFP* (GG)	Assembled by BsaI cut ligation from: LI A-B *pUBi* (G7) + LI dy B-C (G4) + LI A-C *ShRK2* + LI D-E *YFP* (G12) + LI E-F *35S-T* (G59) + LI F-G hygro (G94) + LIIc F 1-2 (BB30)

Plasmids for stable transformation of *A. thaliana*

Name	**Description**
pSEC13:SEC13 + free mCherry	LR reaction of *pENTR-pSEC13:SEC13* and pMDC99 (Curtis & Grossniklaus, 2003); hygromycin resistance
pPOLLUX:POLLUX + free mCherry (GG)	Assembled by BpiI cut ligation from: LII F 1-2 *pPOLLUX:POLLUX* + LII 2-3 ins (BB43) + LII R 3-4 *p35S:mCherry* + LII dy 4-6 (BB41) + LIIIα fin (BB45); kanamycin resistance
pUBi:ShRK1-YFP + free mCherry (GG)	Assembled by BpiI cut ligation from: LII F 1-2 *pUBi:ShRK1* + LII 2-3 ins (BB43) + LII R 3-4 *p35S:mCherry* + LII dy 4-6 (BB41) + LIIIα fin (BB45); hygromycin resistance
pUBi:ShRK2-YFP + free mCherry (GG)	Assembled by BpiI cut ligation from:

	LII F 1-2 *pUBi:ShRK2* + LII 2-3 ins (BB43) + LII R 3-4 *p35S:mCherry* + LII dy 4-6 (BB41) + LIIIα fin (BB45); hygromycin resistance
pUbi:SYMRK-mOrange (GG)	(Antolín-Llovera *et al.*, 2014)

826

827 **S3 Table Oligonucleotides.**

Primer sequences for qPCR-based reverse transcript quantification were taken from these publications

Target	Reference
PP2A	(Czechowski, 2005)
TIP41-like	(Czechowski, 2005)
FRK1	(Asai *et al.*, 2002)
PDF1.2a	(Moffat *et al.*, 2012)
ERF1	(Solano *et al.*, 1998)
PR1	(Onate-Sanchez *et al.*, 2006)

Plasmid construction

Name	Primer sequence (5' - 3')
sec13co_FW	CACCGGGAACACGGGAGAATAG
sec13co_RV	TTTTGCAATCTCTGTTGTCTGA
N133-pro2_FW	AGGGTCTCACACCGTTTTGAAAGACGGCATATTATGG
N133-pro3_RV	AGGGTCTCATACAAGGTCTTTTATTGCTTAAAACTCT
N133-pro3_FW	AGGGTCTCATGTACATTTATTTGTTTTCATTGATTG
N133_Pro4_RV	AGGGTCTCAACATTTTAAACCAGGAAGAGAGCGA
N133_ATG_FW	AGGGTCTCAATGTTCTCTCCATTGACGAAGA
N133_mut_1b_RW	AGGGTCTCATTTCTTTATCCATTCCACCGGA
N133_mut_1_FW	GGGGTCTCAGAAACCTGTCTTTCTTGGTTTATT
N133_mut_2_RW	GGGGTCTCAGCGACCGAGAAGCCCT
N133_mut_2_FW	GGGGTCTCATCGCGTAGTCCTGTTGGTGT
N133_e3_RV	AGGGTCTCACTCTCTGCAGTTGAGTTCCTAGTG
N133_e3_FW	AGGGTCTCAAGAGCCTGCGAACTCTCAAA
N133_3'UTR2_RV	AGGGTCTCACCTTGGTAGATTCGATACATCATAAAGAGG
AtPol-Pro1+	ATGAAGACTTTACGGGTCTCAGCGGAGCCCAATGACTTCCCACAC

AtPol-Pro2-	TAGAAGACAAATGACTACAGTTTCATGCCACCA
AtPol-Pro3+	ATGAAGACTTTCATCATTATGCTCATCTTGAATATGT
AtPol-Pro4-	TAGAAGACAACAGAGGTCTCAGGTGCGGGTTGAAGTAAGTAAATTGAGA
AtPol1+	ATGAAGACTTTACGGGTCTCACACCATGCCGATTCATACCCCTAGA
AtPol2-	TAGAAGACAACATCTTCTTTCTTCTGATTTGTTCGT
AtPol3+	ATGAAGACTTGATGTTCCTTTGAAGAAGAGACTAGC
AtPol4-	ATGAAGACTTCAGAGGTCTCACCTTCTGACTTGAGGCGATGACAAC

828

S4 Table Mutant lines of *A. thaliana* SNUPO genes and seeds used in the study.

Gene and ID	Mutant line	Seedbag
ShRK1 (At1g67720)	GK-699C04 2	1898
ShRK2 (At2g37050)	SALK_143700	1902
ShRK1 (At1g67720) x *ShRK2* (At2g37050)	GK-699C04 2 x SALK_143700	2118
Sec13 (At3g01340) x *Nup133* (At2g05120)	SALK_045825C x SALK_092608C	2130
Nup133 (At2g05120)	SALK_092608C	1941
Pollux (At5g49960)	SALK_066135C	2112
ShRK1 co (At1g67720)	GK-699C04 2 complemented with *pUBi:ShRK1-YFP* + free mCherry	2089
ShRK2 co (At2g37050)	SALK_143700 complemented with *pUBi:ShRK2-YFP* + free mCherry	2079
Sec13 co (At3g01340)	SALK_045825C complemented with *pSEC13:SEC13* + free mCherry	2026
Pollux co (At5g49960)	SALK_066135C complemented with *pPOLLUX:POLLUX* + free mCherry	2149